AD-780 805

IMAGE TRANSMISSION VIA SPREAD SPECTRUM TECHNIQUES

Robert W. Means, et al

Naval Undersea Center

Prepared for:

Advanced Research Projects Agency
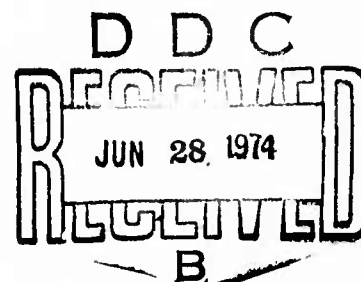
30 June 1974

IMAGE TRANSMISSION
VIA
SPREAD SPECTRUM TECHNIQUES

ARPA Quarterly Technical Report

October 1, 1973 — January 1, 1974

Advanced Research Projects Agency
Order Number 2303
Code Number 3G10

D D C
RECEIVED
JUN 28, 1974
B

Naval Undersea Center
San Diego, California 92132

Approved for Public Release; Distribution Unlimited.

IMAGE TRANSMISSION

VIA

SPREAD SPECTRUM TECHNIQUES

Investigated by
DR. ROBERT W. MEANS (714:225-6872), Code 608
JEFFREY M. SPEISER (714:225-6607), Code 6021
and
HARPER J. WHITEHOUSE (714:225-6315), Code 6003
Naval Undersea Center
San Diego, California

II

ABSTRACT

This paper addresses the design of a spread spectrum image transmission system to provide increased antijam protection to a television link from a small remotely piloted vehicle. Transform encoding and frame rate control may be used to remove the natural redundancy inherent in the image in order to permit the use of spread spectrum encoding for increased antijam protection.

Emphasis is placed on the two-dimensional discrete cosine transform (DCT) and a hybrid DCT with differential pulse code modulation (DPCM). Both the two-dimensional DCT and the hybrid DCT/DPCM provide nearly the theoretically optimal performance of the Karhunen-Loeve transform, while permitting implementation by small, lightweight hardware in real-time.

i

CONTENTS

INTRODUCTION

This program addresses the design of a spread spectrum image transmission system to provide increased anti-jam protection to a television link from a small remotely piloted vehicle. Transform encoding and frame rate control may be used to remove the natural redundancy inherent in the image in order to permit the use of spread spectrum encoding for increased antijam protection.

Previous phases of this program included a study of the performance of one- and two-dimensional transforms, the demonstration of the feasibility of small, lightweight, real-time implementations of the discrete Fourier transform (DFT), and the conceptual design of similar two-dimensional (DFT) implementations.

During the present reporting period, emphasis has been placed on the two-dimensional discrete cosine transform (DCT) and a hybrid DCT with differential pulse code modulation (DPCM). Both the two-dimensional DCT and the hybrid DCT/DPCM provide nearly the theoretically optimal performance of the Karhunen-Loeve transform, while permitting implementation by small, lightweight hardware in real-time.

The conceptual design of the two-dimensional DCT has been completed, but its further evaluation awaits the development of a random access sensor with nondestructive readout.

The hybrid DCT/DPCM is compatible with present sensors and therefore the most promising transform for use in the immediate future.

SYSTEM DESCRIPTION

Two hybrid cosine-DPCM bandwidth reduction systems have been selected for construction and evaluation. The first uses a Charge Injection Device (CID) [1] image sensor and a Bucket Brigade Device (BBD) transform implementation. The second uses an ordinary vidicon sensor and a Charge Coupled Device (CCD) transform implementation.

In the CID system a 100x100 pixel solid state sensor will be used. The nominal horizontal line scan will be one millisecond. The nominal frame rate will be 10 frames per second which can be displayed without flicker through the use of a scan converter. The 1 millisecond line scan time was chosen in order to match the sensor to the BBD filter which operates at a clock rate of 100 kHz with good charge transfer efficiency. At 10

frames per second, image motion should be reproduced well even though some picture detail will be lost because of the low spatial sampling afforded by the 100x100 pixel format.

When the cosine transform in the horizontal direction is combined with Differential Pulse Code Modulation (DPCM) in the vertical direction to form a hybrid transform system, performance essentially indistinguishable from "optimum" Karhunen Loeve should be achieved as shown in Appendix A. Minimum overall bit rate will be achieved by a combination of zonal filtering and variable bit assignment with low spatial frequencies assigned more bits of quantization than high spatial frequencies. Table 1 shows the bit rate which results from three overall bits/pixel assignments at a pixel rate of 10^5 pixels/sec. An overall bit assignment of 1 bit/pixel should result in a signal-to-distortion ratio of better than 30 dB. In addition, since channel errors occur in the Fourier domain, channel error rates as large as $P=10^{-2}$ will still provide useful reconstructed images.

The second bandwidth reduction system will be compatible with a standard vidicon camera. It will use CCD filters for the cosine transform which will operate at a 4.8 MHz sampling rate. Compatibility with standard television format will be maintained in as many aspects as possible. Thus 53.5 microseconds of every line scan will be used for video data transmission and 10 microseconds of every line will be reserved for special functions such as synchronization. If the interlace field is used directly as the input to the transform hardware a resolution of approximately 240 lines by 256 pixels is possible at 60 frames/second. This is equivalent to a video bandwidth slightly less than 2.5 MHz. However, in order to reduce the effective frame rate, a block of 32 adjacent pixels will be used. Thus if every other 32 pixels of each line were transformed, it would result in a horizontal interlace and an equivalent frame rate of 30 frames/sec. Slower frame rates can be achieved

Table 1. Bit Rate as a Function of Quantization for the
CID System

Bits/Pixel	Bit Rate
2	200 kilobits/sec
1	100 kilobits/sec
1/2	50 kilobits/sec

2

by deleting additional 32 pixel blocks until a minimum frame rate of 7.5 frames/sec is achieved when only one 32 pixel block per line is used.

The number of pixels per frame is 61440. Table 2 shows the bit rate which results at several frame rates and bits/pixel.

Table 2. Bit Rate as a Function of Quantization and Field
Rate for the Vidicon Compatible System.

Bits/Pixel	Field Rate (fields/sec)	Bit Rate (kilobits/sec)
1	30	1843.2
1	15	921.6
1	7.5	460.8
1/2	30	921.6
1/2	15	460.8
1/2	7.5	230.4

SPREAD SPECTRUM ENCODING

The amount of anti-jam capability of the system will depend on the subsequent coding algorithm used to encode the data. A relative compression ratio (in dB) can be defined for use in comparing various bandwidth compression schemes

$$C. R. \equiv 10 \log \left(\frac{\text{channel bit rate}}{N*B*F} \right)$$

where N is the number of pixels per video frame, B is the number of quantization bits per pixel and F is the frame rate. The channel bit rate is assumed to be 20.0 megabits per second.

The compression ratio is, in a sense, an approximate lower bound on the amount of anti-jam capability available by a not very sophisticated coding scheme. A bit stream repetition would be one such naive scheme. A candidate scheme to use maximal length PN cyclic codes to spread the spectrum appears to offer significant improvements over naive schemes.

3

Consider the conventional vidicon system in which it is planned to transmit 32 pixels out of every line for an effective frame rate of 7.5 frames/sec. A length 1023 PN sequence sent at a 20 megabit rate occupies 51.15 μs leaving 12.3 μs for a coded sync pulse. A cyclic 1023 bit PN sequence can transmit 10 bits of information via cyclic pulse position modulation. This corresponds to 27.1 dB of anti-jam protection as measured by the increased distance between code words as compared to a direct binary transmission. However we have only transmitted an average of 0.312 bits/pixel. An alternative would be to break the 1023 bit sequence into two sequences of length 511 each lasting 25.6 μs. Each one carries 9 bits of information for a total of 18 bits and an average of .563 bits/pixel at 24.1 dB anti-jam protection. This is further illustrated in table 3. As can be seen from this table a sophisticated coding scheme gives approximately a 5 dB benefit in AJ. Consider the same situation for the 100x100 pixel charge coupled device camera. If length 1023 PN sequences are clocked at 20 megabits per second twenty 51.15 microsecond periods could be used per line to produce a frame rate of about 10 per second. Performance versus codeword length is summarized in Table 4. The additional anti-jam benefit from the coding scheme gives the CID camera the capability of running at a higher frame rate than that given in Table 4 and still achieving good picture quality and good AJ capability. Table 5 summarizes the performance for a 30 frame/sec system. Since this system is capable of operating at 30 frames per second with good AJ and good picture quality (27.1 dB AJ at 1.08 bits/ pixel), it offers the possibility of eliminating a potentially costly scan converter at the ground station. The picture is however, either of lower resolution or of smaller field of view than the vidicon system.

Table 3. AJ Improvement for Vidicon Compatible System Using PN-PPM

Length of the Sequence	No. of Sequences Transmitted	Decoded Bits per Sequence	Total No. of Bits	Average Bits per Pixel	AJ (dB)	CR (dB)
1023	1	10	10	0.31	27.1	21.4
511	2	9	18	0.56	24.1	18.9
255	4	8	32	1.0	21.1	16.4
127	8	7	56	1.75	18.1	13.9

4

Table 4. Performance vs. Codeword Length for the CID
System at 10 Frames/sec Using PN-PPM.

Length of the Sequence	No. of Sequences Transmitted	Decoded Bits per Sequence	Total No. of Bits	Average Bits per Pixel	AJ (dB)	CR (dB)
1023	20	10	200	2.0	27.1	20.0
511	40	9	360	3.6	24.1	17.4
255	80	8	640	6.4	20.1	14.9

Table 5. Performance vs. Codeword Length for the CID
System at 30 Frames/sec Using PN-PPM.

Length of the Sequence	No. of Sequences Transmitted	Decoded Bits per Sequence	Total No. of Bits	Average Bits per Pixel	AJ (dB)	CR (dB)
1023	6	10	60	0.6	27.1	21.2
511	12	9	108	1.08	24.1	17.9
255	24	8	192	1.92	21.1	15.4

DPCM TRANSFORM IMPLEMENTATION

For television bandwidth reduction, it has been shown [2, 3] that a two-dimensional mixed transform, e.g. Fourier in the horizontal direction and Hadamard in the vertical direction, generally gives performance intermediate between the two transforms. An exception to this generalization is the DPCM transform. The combination of the cosine transform in the horizontal direction and the DPCM transform in the vertical direction has performance equivalent to the optimal Karhunen Loeve transform as shown in Appendix A.

This result has been demonstrated both theoretically and by computer simulation. A hardware DPCM system has been designed and is being constructed. It is meant to interface with a slow scan television system such as the new 100 x 100 charge coupled device cameras now entering the market. A block diagram of the DPCM system is shown in Figure 1.

The DPCM has been designed with a sixteen level nonlinear quantizer representing three bits of magnitude information and one bit of sign information. The quantization
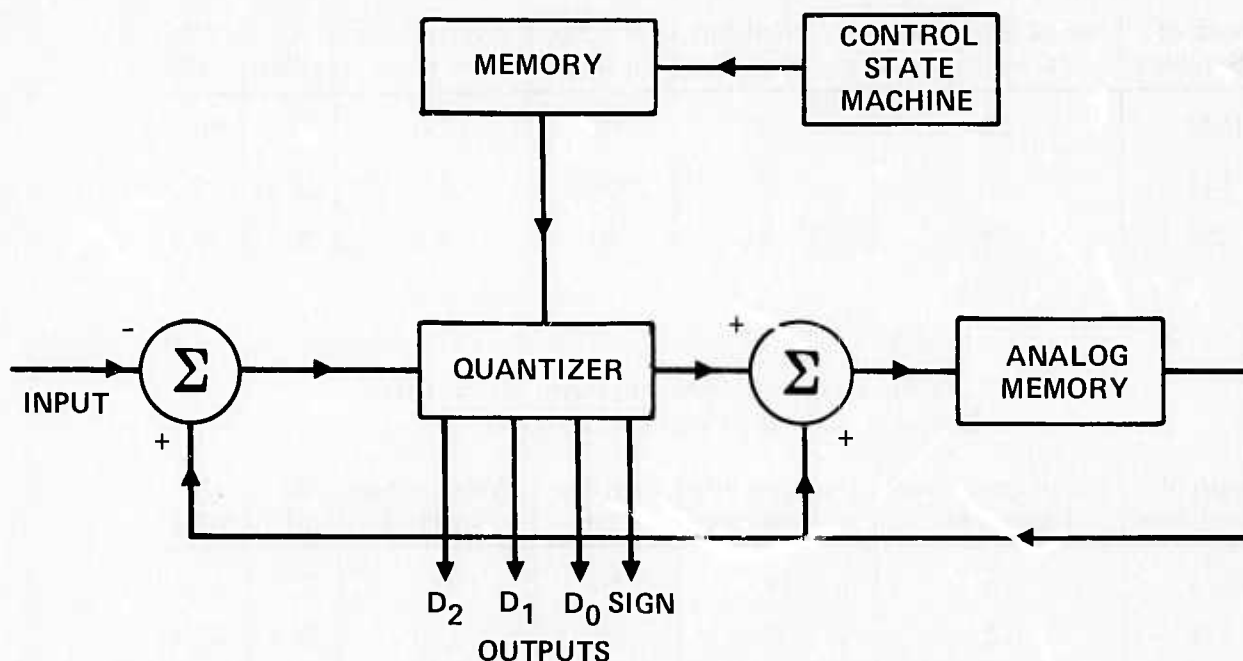
5

Figure 1. The DPCM System.

levels can be set to arbitrary levels. Zero, two, three or four bits of information can be transmitted per coefficient depending on a command from a memory unit. The memory unit is programmable and allows the operator to adjust the number of bits per coefficient to the coefficient location. The system is also designed to give the operator control of the number of coefficients sent. The analog memory is being simulated by an A/D converter, a set of digital shift registers and a D/A converter. An appropriate charge coupled device analog memory is not available at the present time. From the experience gained in the design of this DPCM encoder it appears that an all digital DPCM system (except for the initial summing amplifier) would be the simplest type to construct and has significant power and weight advantages over a hybrid encoder.

6

IMPLEMENTATION OF ONE- AND TWO-DIMENSIONAL
DISCRETE COSINE TRANSFORMS

Emphasis has been placed on the implementation of the discrete cosine transform (DCT) because it provides a very close approximation to the optimum Karhunen-Loeve transform, while permitting compact, real-time implementation by a combination of multipliers and filters. The two types of DCT which are useful for reduced redundancy television image transmission are obtained by extending a length N data block to have even symmetry, taking the discrete Fourier transform (DFT) of the extended data block, and saving N terms of the DFT.

The "Odd DCT" (ODCT) extends the length N data block to length 2N–1 and the "Even DCT" extends the length N data block to length 2N. For example, if the data block were ABC, the two extensions would be CBABC and CBAABC, respectively. Analytic expressions for these transforms are given in Appendix B.

An ODCT or EDCT in the horizontal direction may be combined with an ODCT or EDCT in the vertical direction to give three different types of two-dimensional DCT.

Three different ways of implementing a one-dimensional DCT in real time have been found, requiring filter lengths of approximately 4N, 2N, and N for an N-point transform. A detailed comparison is provided in Table 1 of Appendix B.

Two of the three types of two-dimensional DCT may also be implemented in real-time using combinations of multipliers and filters. The image points may be scanned so as to produce a one-dimensional sequence whose one-dimensional transform is the required two-dimensional DCT of the image as described in Appendix B and illustrated in Tables 2 and 3 of that appendix. If the horizontal and vertical sizes of the extended data block have no common divisor, then the two-dimensional DFT required for a two-dimensional DCT may be performed as a one-dimensional DFT by suitably scanning the extended data block by re-scanning the original data block.

The choice of a hybrid ODCT by even DCT permits maximum flexibility in the block size, since any square block size may be used, and the two-dimensional transform may be implemented using the switching filter EDCT, shown in Figure 3 of Appendix B, to maximize the block size attainable with a limited number of taps per filter. In this case, filters

of length $N_2(2N_1-1)$ will be needed for a block size of N_1 by N_2, so that a two-dimensional DCT of a 10 by 10 data block is within the limits of present bucket brigade device filters.

REPORT SUMMARY

This report describes the progress on the third phase of a NUC program on image bandwidth reduction for application to the ARPA RPV problem of sending television images over spread spectrum channels. This report details the second quarter of a hardware development and implementation phase. In this quarter implementation and interfacing were considered for the two-dimensional DCT and hybrid DCT/DPCM which were previously shown to provide nearly optimum performance.

Two-dimensional discrete cosine transform implementations have been designed, but their utilization awaits development of a compatible sensor. Two-dimensional hybrid DPCM/DCT transform hardware is being built, and a suitable pseudonoise pulse position coding format has been shown to maximize the minimum distance between code words and to provide a significant increase in AJ protection compared to simple bit stream repetition. The improvement is about 5 dB for a codeword size of 511 bits with a compression ratio of 78 to 1 and is a slowly varying function of the compression ratio. The coding format is compatible with transmission through either an analog or a binary channel.

REFERENCES

[1]   Michon, C. J. and Burke, H. N., "Operational Characteristics of CID Imager," *ISSCC Digest of Technical Papers*, p. 26-27; Feb, 1974.

[2]   R. W. Means and H. J. Whitehouse, *Image Transmission via Spread Spectrum Techniques*, ARPA Quarterly Technical Report, June 1973, Order Number 2303, Code Number 3610.

[3]   R. W. Means, J. M. Speiser and H. J. Whitehouse, *Image Transmission via Spread Spectrum Techniques*, ARPA Quarterly Technical Report, October 1973, Order Number 3610.

APPENDIX A

REAL TIME IMAGE REDUNDANCY REDUCTION USING
TRANSFORM CODING TECHNIQUES

Ali Habibi
William K. Pratt
Guner Robinson
University Of Southern California

Robert W. Neens
Harper Whitehouse
Jeffrey Speiser
Naval Undersea Center

REAL TIME IMAGE REDUNDANCY REDUCTION USING TRANSFORM CODING TECHNIQUES[*]

Ali Habibi   William K. Pratt   Guner Robinson   Robert Means   Harper Whitehouse   Jeffrey Speiser

Electrical Engineering Department
Image Processing Institute
University of Southern California
Los Angeles, California 90007

Naval Undersea Center
San Diego, California 92132

ABSTRACT

Several image coding systems based upon transform coding have been studied. Analysis and simulation has shown that in many applications these systems are capable of image coding at about one to two bits per pixel with acceptable image quality and tolerance to channel errors. Implementation studies and tests that have been performed indicate that the systems can be implemented for real time television operation using recently developed technologies.

INTRODUCTION

Transform coding techniques have been explored extensively in theoretical studies and by simulation. It has been shown that a significant bandwidth reduction can be achieved in many applications with minimal image degradation and relative tolerance to channel errors. The major drawback of transform image coding for real time television applications in the past has been computational complexity. However, recently developed technologies such as acoustic surface wave delay lines and charge coupled devices have made transform image coding at real time television rates feasible.

CODING TECHNIQUES

Transform Coding.[1]

In transform coding systems a one or two dimensional mathematical transform of an image line segment or block is performed at the coder. The transform coefficients are then quantized and coded. At the receiver, after decoding, an inverse transform is taken to obtain an image reconstruction. Transforms that have proven useful include the Fourier, Hadamard, Slant, Cosine, and Karhunen-Loeve transforms. A bit rate reduction is obtained by efficient quantization and coding of the transform coefficients. Many of the transform coefficients of a natural image are of relatively low magnitude and can be discarded entirely, or coded with a small number of bits per coefficient while maintaining a small mean square error. Simulation studies indicate that a bit rate reduction to about 1.5 bits/pixel can be obtained for monochrome image transform coding in 16 X 16 pixel blocks. Color images require about 2.0 bits/pixel. Figure 1 shows an original and encoded pictures for two-dimensional transform coding in 16 X 16 pixel blocks at bit rates of 0.5 and 1 bit per pixel.

DPCM Coding.[2]

In a DPCM system the value of a scanned image sample is predicted and the difference between the actual and the predicted value is quantized and transmitted. At the receiver a similar predictor uses transmitted values of the quantized differential signal to reconstruct a replica of the scanned image. Prediction of a data point is performed by using a number of adjacent previously scanned sample values where the parameters of the predictor are specified in terms of the correlation of picture elements.

Properties of the differential signal that make a DPCM system attractive are a significant reduction in the variance of the differential signal, as compared to the variance of the original samples, and the fact that the probability density function of the differential signal is closely approximated by an exponential function.[3] The former

(a) Original

(b) 0.5 Bits/Pixel

(c) 1 Bit/Pixel

Fig. 1. Original and encoded signal using two-dimensional cosine transform and block quantization.

property results in smaller quantization noise power, while the latter property allows for designing an optimum quantizer to obtain a further reduction of noise power. Besides these two improvements, the quantized differential signal has a smaller entropy than the quantized original signal. This results in further bandwidth reduction (or equivalently improvements in signal to noise ratio) if the transmitted signal is entropy coded. With standard DPCM systems, monochromes images are coded with 2.5 to 3.0 bits/pixel.

Comparison of Transform and DPCM Coding.[3]

Both DPCM and the transform coding techniques have been used with some success in coding pictorial data. A study of both these systems has indicated that each technique has some attractive characteristics and some limitations. Transform coding systems: (a), achieve superior coding performance at lower bit rates; (b), distribute the coding degradation in a manner less objectionable to a human viewer; (c), show less sensitivity to data statistics (picture-to-picture variation); and (d), are less vulnerable to channel noise, compared to DPCM coding systems. On the other hand, DPCM systems, when designed to take advantage of spatial correlations of the data: (a), achieve a better coding performance at a higher bit rate; (b), require less complex coding equipment; (c), produce a minimal coding delay; and (d), do not require a large block memory, as compared to transform coding systems.

Hybrid Transform/DPCM Coding.

A serious shortcoming of two-dimensional transform encoders is the requirement of a block memory. To avoid this problem and yet retain the attractive features of transform coding systems, a hybrid encoder that uses a cascaded unitary transformation, DPCM encoder has been developed. The hybrid encoder, shown on Figure 2, exploits the correlation of the data in the horizontal direction by taking a one-dimensional transform of each line of the picture, then it operates on each column of the transformed data using a bank of DPCM coders. The DPCM coders replace the quantizers in a two-dimensional transform coding system. Since the unitary transformation involved is a one-dimensional transformation of individual lines of the pictorial data, the equipment complexity and the number of computational operations is considerably less than for a two-dimensional transformation.

The hybrid system concept can be extended to interframe coding of television signals. Such a coding system would start by taking a two-dimensional transformation of each block of the television signal, then it would encode the transformed signal in the temporal direction by a number of parallel DPCM encoders, thus exploiting the correlation of data in temporal as well as spatial directions.

Both theoretical and the experimental results indicate that a hybrid system employing a Karhunen-Loeve transformation produces a better result than a hybrid system using any other unitary transformation. The theoretical results for Markov data, summarized in Figure 3, also show that the performance of the Cosine transform system is only slightly suboptimum to the Karhunen-Loeve transformation system, and is superior to the hybrid Hadamard or Fourier transform systems. As an illustration of performance, Figure 4 contains encoded pictures for a hybrid transform/DPCM coder.

To evaluate the effect of a noisy transmission link, hybrid coded images have been subjected to a simulated binary symmetric channel with a probability of bit reversal equal to p. It has been found that the inherent error propagation in the DPCM systems of the hybrid coder can be reduced considerably by using a smaller value for the A_i's shown in Figure 2. Naturally, the best value for the A_i's depends upon the bit error probability p. For $p = 10^{-2}$ a value of $A_i = 0.8$ gives near optimal results. Figure 4a and 4b show encoded pictures for a hybrid coder with $A_i = 0.8$ for a probability of error of $p = 10^{-2}$.
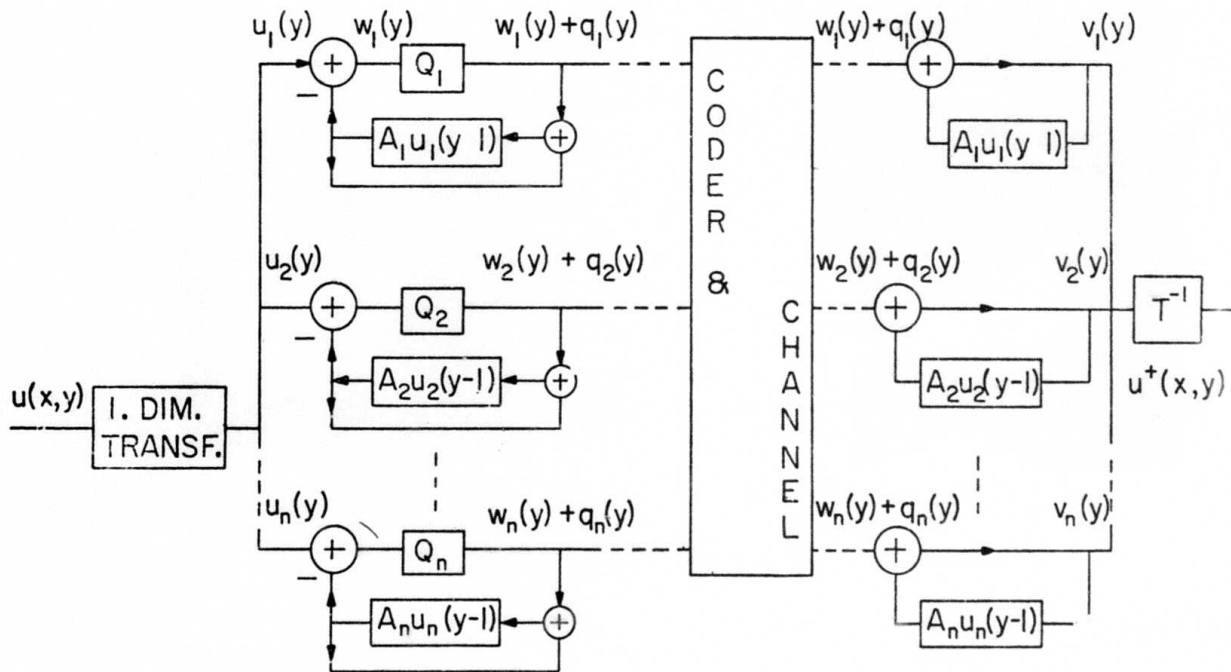
Fig. 2. Block diagram of the hybrid system using a cascade of one-dimensional transformations and a bank of DPCM systems to encode pictorial data.
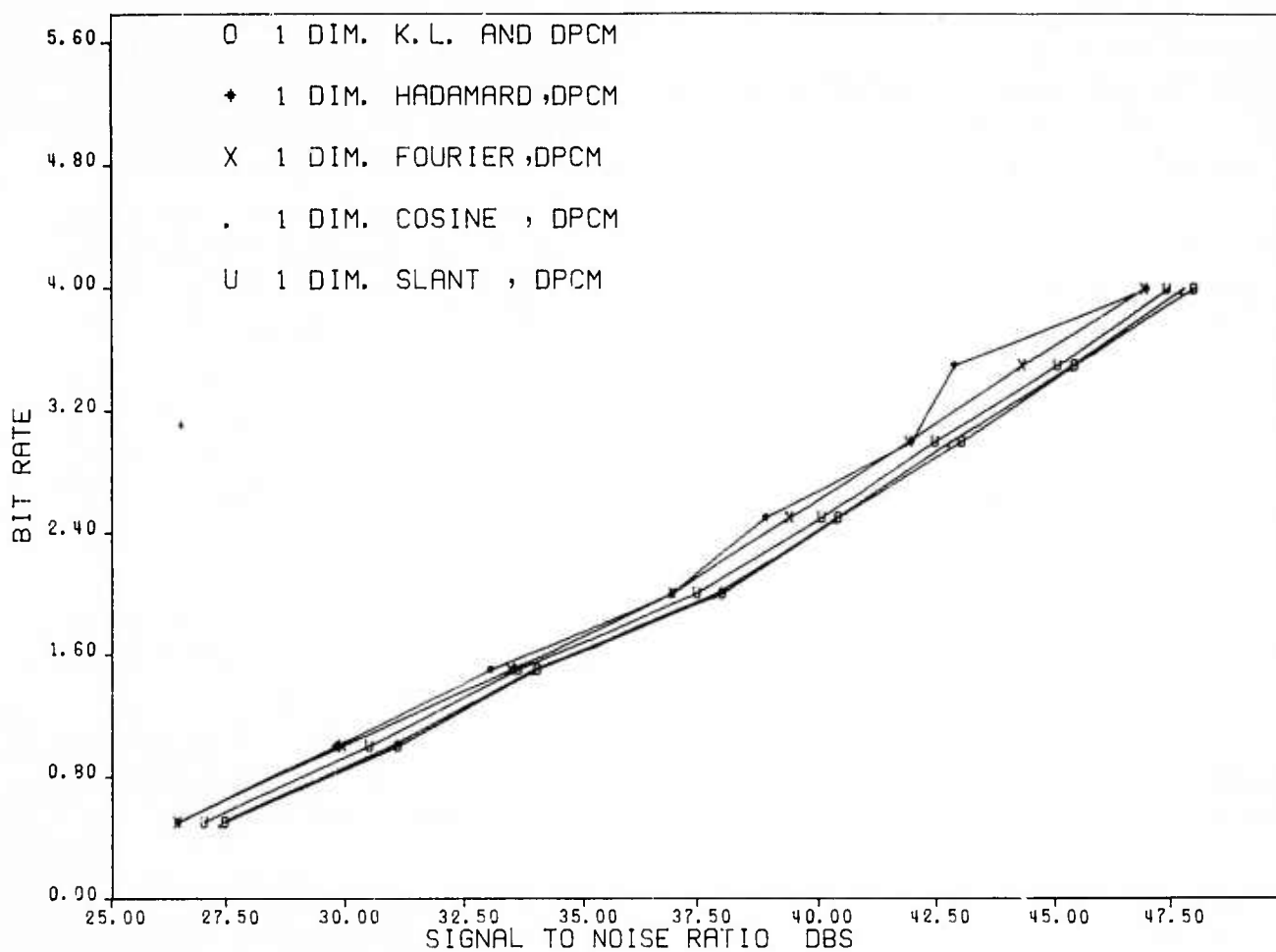
Fig. 3. Bit rate versus the signal-to-noise ratio for the proposed one-dimensional hybrid systems for the discrete random field.

(a) 0.5 Bit/Pixel
    $p = 10^{-2}$

(b) 1.0 Bit/Pixel
    $p = 10^{-2}$

Fig. 4. Encoded pictures using the hybrid encoder (cosine transform and DPCM).

A-4

TRANSFORM CODING QUANTIZATION ERROR REDUCTION[4]

In transform coding systems a bandwidth reduction is achieved by coarsely quantizing the transform coefficients. This, of course, introduces an error in reproduction. It is possible, however, to compensate for quantization error at the receiver in many applications and obtain an improvement in image quality.

Consider an N element vector $\underline{f}$ that represents the pixels in an image block. The transform coefficients of the image block are given by the N element vector

$$\underline{f} = \underline{A}\,\underline{f}$$

where $\underline{A}$ is an N X N unitary transformation matrix. For purposes of analysis assume $\underline{f}$ is a sample of a zero mean random process with known covariance matrix $\underline{K}_f$. Then the covariance matrix of the transform coefficients is

$$\underline{K}_f = \underline{A}\,\underline{K}_f\,\underline{A}^{-1}$$

If a Karhunen-Loeve transform is employed, all transform coefficients are uncorrelated, and $\underline{K}_f$ becomes an identity matrix. For all other transforms, there is some residual correlation between coefficients that can be exploited to reduce quantization error.

Now let $\underline{f}_Q$ denote the N element vector of quantized coefficients that are coded, transmitted, and eventually reconstructed at the receiver. In most transform coding systems, the vector of quantized transform coefficients is simply inverse transformed to reproduce a vector of reconstructed image pixels, $\hat{\underline{f}}$. The resulting mean square coding error is

$$\delta = \mathrm{tr}\left[E\{ (\underline{f}-\hat{\underline{f}})(\underline{f}-\hat{\underline{f}}^T\} \right]$$

It is possible to reduce the mean square error by introducing a linear smoothing of the quantized transform coefficients. Let

$$\underline{f} = \underline{W}\,\underline{f}_Q$$

denote the result of the smoothing process where $\underline{W}$ is the smoothing operator matrix. The reconstructed vector of image pixels is then

$$\underline{f} = \underline{A}^{-1}\hat{\underline{f}}$$

Considerable study has been performed to develop smoothing operators $\underline{W}$ which reduce the mean square coding error, but yet are computationally feasible. Details are available.[4] As an example of the potential of this technique Figure 5 shows the result of transform domain quantization error reduction applied to the Hadamard transform of an image in 16 X 16 pixel blocks. In these simulations the lowest spatial frequency transform coefficients in a 5 X 5 element block were finely quantized so that their quantization error was negligible. The remaining coefficients were discarded. At the receiver the missing coefficients were estimated from the received coefficients before the inverse transformation. The reconstructions with and without the quantization error reduction graphically indicate the image quality improvement possible with this technique.

TRANSFORM IMPLEMENTATION

The major difficulty in implementing transform coding or hybrid transform coding with DPCM in real time has been the large number of multiplications required by the transforms which provide the best coding performance. Since a tapped delay line transversal filter provides serial access memory together with the equivalent of a large number of multipliers operating in parallel, it provides the possibility of performing most of the needed multiplications in the memory which stores the data block. One-dimensional and two-dimensional discrete Fourier transforms and discrete cosine transforms lend themselves well to such an implementation, and a real-time implementation of a close approximation to the optimum Karhunen-Loeve transform is therefore possible for moderate block sizes.

One Dimensional Transforms.

The discrete Fourier transform (DFT) is well suited for use in real-time image processing since it is asymptotically close to the Karhunen-Loeve transform and can be implemented by a combination

Original

10:1 Zonal Selection

10:1 Zonal Selection
Spectrum Extrapolation

Fig. 5. Hadamard Spectrum Extrapolation

of multipliers and filters. In one dimension the DFT of a complex vector g composed of N samples is given by

$$G_k = \sum_{n=0}^{N-1} g_n \exp\{-i2\pi nk/N\} \qquad (1)$$

or

$$G_k = \exp\{-i\pi k^2/N\} \sum_{n=0}^{N-1} \exp\{i\pi(n-k)^2/N\}\exp\{-i\pi n^2/N\}g_n \quad (2)$$

through the use of the substitution $2nk = n^2 + k^2 - (n-k)^2$. This Chirp-Z-transform (CZT) representation of the DFT can be interpreted

as a multiplication of the vector to be transformed by a discrete chirp, periodic convolution of the multiplied vector by a discrete chirp, and post multiplication by a discrete chirp.[6]

Equation (2) may be implemented using real multipliers and real filters. This configuration is shown in Figure 6. With the further restriction that the function g is real, non-negative and even, G is real and is an autocorrelation function. For an image vector of size N there are two symmetrized extensions of the vector; the first of size 2N, the other of size 2N-1. Corresponding to the DFT of these two extended vectors there are two discrete cosine transforms (DCT)

$$G_{ek} = 2 \sum_{n=0}^{N-1} g_n \cos \pi (n+1/2) k/N \qquad (EDCT) \qquad (3)$$

$$G_{ok} = g_0 + 2 \sum_{n=0}^{N-1} \cos \pi nk/(N-1/2) g_n \qquad (ODCT) \qquad (4)$$

Since the DFT is equivalent to the Fourier transform of a periodic repetition of the data vector, symmetrizing the input signal improves the convergence at any light-dark edge discontinuities of the periodic extension. In addition, for images with exponential correlation functions Ahmed[5] has shown that the EDCT is almost indistinguishable from the Karhunen-Loeve transform.

However, it is in hardware implementation that the DCTs excel since they may be computed simply as the real part of a DFT via the CZT algorithm. The CZT algorithm is a "real-time" algorithm which makes it possible to compute, in natural frequency order, Fourier coefficients at the same rate as the data is being gathered. In addition, the computation involves only multiplication and convolution which can be performed by analog multipliers and linear filters respectively. Thus analog to digital conversion of the video is not required nor is there a need for special purpose digital computations.

Two technologies are available for the implementation of the convolution filters: surface acoustic waves (SAW) and charge transfer devices (CTD). The SAW technology uses acoustic waves on piezoelectric crystals with deposited electrodes while the CTD uses an electric field to induce propagation of concentrations of minority carriers at a silicon-silicon oxide boundary in a monolithic silicon analog integrated circuit. In both technologies the required linear filters are

implemented as transversal filters whose impulse responses are determined by the metalization pattern deposited during fabrication.

The transversal filter was first proposed by Kallmann[7] and consists of a non-dispersive delay line contiguously tapped along its length transverse to the direction of signal propagation with lightly coupled non-interacting taps. The impulse response of this filter is uniquely specified by the amplitude and polarity of the taps and any bounded, finite duration impulse response of specified bandwidth can be synthesized by sampling the desired response signal at its Nyquist rate and setting the tap weights along the delay line to these values. Although a transversal filter normally implements a non-periodic convolution, periodic convolution can be achieved by a number of techniques: (1) the input signal can be repeated; (2) the output of the delay line can be recirculated to the input; (3) the impulse response can be made two periods of the desired function; or (4) an auxiliary delay line can be employed.

In order to continuously transform the input signal, this signal must be subdivided into blocks whose lengths are the same size as the size of the appropriate Fourier transform and two sets of convolution filters used alternately. However, the pre- and post-multipliers may be multiplexed between the two groups of filters. By these techniques a $\log_2 N$ increase in throughput is possible over a corresponding fast Fourier transform (FFT) operating at the same sample rate and employing one complex multiplier. This results in a reduction of size and power since no quantization is required and calculation proceeds at the data sample rate.

When a vertical differential pulse code modulator (DPCM) modem follows a horizontal cosine transform a very compact digital real-time image transmission system results. As shown in part 2, this system achieves performance essentially indistinguishable from that of the Karhunen-Loeve transform for pictures with exponential correlation functions without having to employ two dimensional transform encoding. However, if two dimensional Fourier encoding is required it may be achieved by concatenation of two one dimensional transforms with auxiliary memory to transpose the partial transform from row to column format; or it may be achieved by linear congruential scanning of the two dimensional area and the use of a one dimensional transformation as described under two dimensional transforms.
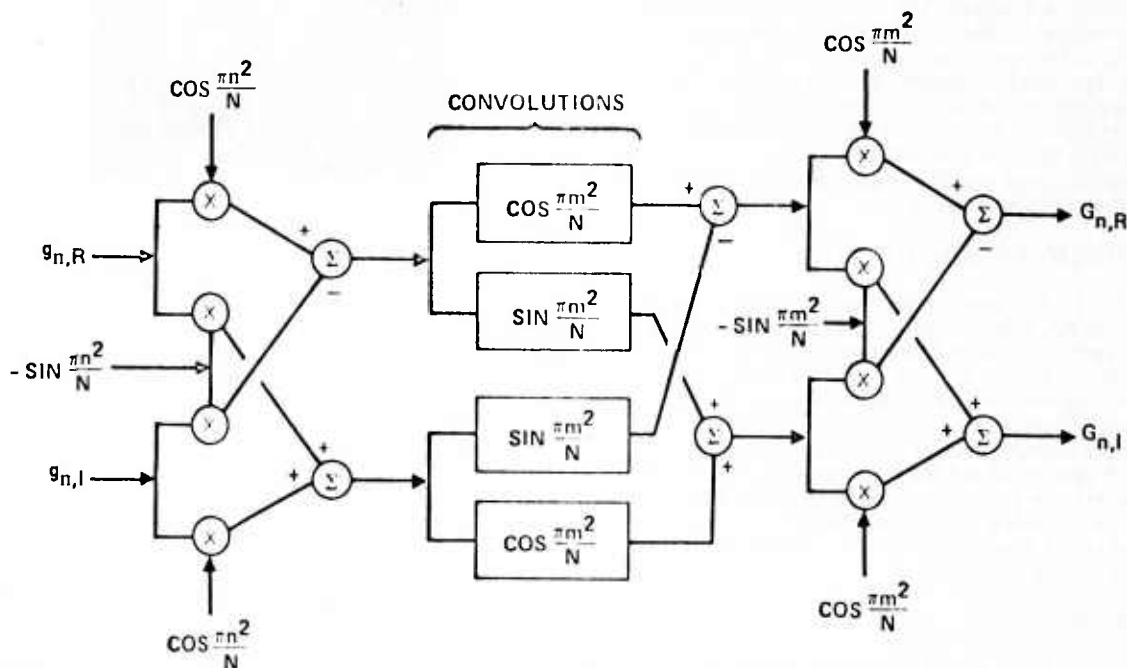

Fig. 6. DFT via CZT algorithm with parallel implementation of complex arithmetic.

A-6

Two Dimensional Transforms

The alternative expressions for the ODCT and EDCT shown in eqs. (5) and (6) make evident their implementation. The appropriate premultiplier reference function, transversal filter tap weights and postmultiplier reference function for the ODCT and EDCT are given by a, b, c of eqs. (7) and (8) respectively.

$$G_{ok} = 2\,Re\left[\exp\left\{\frac{-i\pi k^2}{2N-1}\right\}\sum_{j=0}^{N-1} s_j\,g_j\,\exp\left\{\frac{i\pi j^2}{2N-1}\right\}\right.$$

$$\left.\exp\left\{\frac{i\pi(k-j)^2}{2N-1}\right\}\right] \tag{5}$$

where $s_0 = .5$ and $s_m = 1$ for $j > 0$

$$G_{ek} = 2\,Re\left[\exp\left\{\frac{-i\pi(k^2+k)}{2N}\right\}\sum_{j=0}^{N-1} g_j\,\exp\left\{\frac{-i\pi j^2}{2N}\right\}\right.$$

$$\left.\exp\left\{\frac{i\pi(k-j)^2}{2N}\right\}\right] \tag{6}$$

For the ODCT

$$a_j = \begin{cases} .5, & j=0 \\ \exp\left\{\dfrac{-i\pi j^2}{2N-1}\right\}, & j=1,\dots N-1 \end{cases} \tag{7A}$$

$$b_j = \exp\left\{\frac{i\pi j^2}{2N-1}\right\},\ \text{for } j = -(N-1),\dots (N-1) \tag{7B}$$

$$c_j = \exp\left\{\frac{-i\pi j^2}{2N-1}\right\},\ \text{for } j = 0,\dots N-1 \tag{7C}$$

For the EDCT

$$a_j = \exp\left\{\frac{-i\pi j^2}{2N}\right\},\ \text{for } j=0,\dots N-1 \tag{8A}$$

$$b_j = \exp\left\{\frac{i\pi j^2}{2N}\right\},\ \text{for } j = -(N-1),\dots (N-1) \tag{8B}$$

$$c_j = \exp\left\{\frac{-i\pi(j^2+j)}{2N}\right\},\ \text{for } j=0,\dots N-1 \tag{8C}$$

A two-dimensional DFT of an M_1 by M_2 data block may be performed as a one-dimensional DFT of size $M = M_1 M_2$ of a sequence obtained by an appropriate linear congruential scan of the data block provided that M_1 and M_2 have no common divisor.[8,10]

The equivalent two and one dimensional DFTs are given in eqs. (9) and (10) respectively, with the input scan defined by eqs. (11) and (12), and the output scan defined by eqs. (13) and (14). The constants $u_1, v_1 \cdot u_2, v_2$ may be any solutions of eqs. (15) and (16).

$$G(k_1,k_2) = \sum_{j_1=0}^{M_1-1}\sum_{j_2=0}^{M_2-1} g(j_1,j_2)$$

$$\exp\left\{-i2\pi\left[\frac{j_1 k_1}{M_1} + \frac{j_2 k_2}{M_2}\right]\right\} \tag{9}$$

$$\text{for}\quad k_1 = 0,\dots M_1-1$$
$$k_2 = 0,\dots M_2-1$$

$$F_q = \sum_{p=0}^{M-1} f_p\,\exp\left\{\frac{-i2\pi pq}{M}\right\}$$

$$\text{for } q = 0,\dots M-1 \tag{10}$$

$$p(j_1,j_2) = j_1 u_1 M_2 + j_2 u_2 M_1 \qquad (MOD\ M) \tag{11}$$

$$f_p = g(j_1,j_2) \tag{12}$$

$$q(k_1,k_2) = k_1 v_1 M_2 + k_2 v_2 M_1 \qquad (MOD\ M) \tag{13}$$

$$F_q = G(k_1,k_2) \tag{14}$$

$$M_2 u_1 v_1 = 1 \qquad (MOD\ M_1) \tag{15}$$

$$M_1 u_2 v_2 = 1 \qquad (MOD\ M_2) \tag{16}$$

The incorporation of a two-dimensional DFT device using the linear congruential scan into a reduced redundancy image transmission system is shown in Figure 7. Since unequal quantization would normally be applied to the transform output values, the output scan coordinates available at B and C may be used to keep track of the coordinates of the output value at A.

A two-dimensional DCT of an N_1 by N_2 data block may be regarded as a two-dimensional DFT of an M_1 by M_2 data block, where $M_k = 2N_k$ or $M_k = 2N_k-1$ depending on whether an EDCT or an ODCT is used in the kth direction. If M_1 and M_2 have no common divisor, the two-dimensional DCT may therefore be performed as a one-dimensional DFT using CZT hardware. The configuration of Figure 8 is therefore appropriate for the two dimensional DCT as well as the two-dimensional DFT. For the two-dimensional DCT, however, the extended data block is scanned by an appropriate rescan of the original data block, and a modified scan generator will be needed. In addition, the one-dimensional DFT size needed to perform a two-dimensional DCT in this way is $M_1 M_2$, which is almost four times larger than $N_1 N_2$. If the symmetry of the one-dimensional sequence generated by the linear congruential scan of the extended data block is exploited, the length $M_1 M_2$ one-dimensional DFT may be replaced by a one-dimensional DCT of about half that length, thus permitting a substantial reduction in the number of taps needed in the filters.

Transform Hardware.

This section will describe how both surface acoustic wave devices and charge transfer devices have been used to implement the chirp-Z algorithm for bandwidth reduction.[9,10] The surface acoustic wave system was constructed to be compatible with standard television. The charge transfer device system was constructed to be compatible with a slow scan television camera such as the new 100×100 charge coupled device cameras now on the market. A second charge transfer device system is being constructed to be compatible with standard television.

A block size of 32 has been chosen for a feasibility demonstration of a surface acoustic wave implementation of the real-time discrete Fourier transform. With a conventional line scan time of 53.5 microseconds and a sample rate of 256 samples per line, a 4.78 MHz sampling rate is required. A block of 32 points transforms 6.69 microseconds or one eighth of the video signal. The total number of taps on the filter is 63, i.e., 2N-1. Two SAW devices have been constructed at the Naval Undersea Center. One is used to generate the 32 point sine and cosine chirp signals for pre- and postmultiplication. The other is used to convolve the multiplied input with the four transversal filters as shown in Figure 6. A photograph of the SAW device in shown in Figure 8.

The feasibility of the charge transfer device implementation has been demonstrated with a bucket brigade transversal filter. The bucket brigade devices have 200 taps and can operate at a sampling rate of several hundred kilohertz. This makes them ideal for slow scan, low resolution TV such as the recent 100×100 charge coupled device cameras. The tap weights of the bucket brigade device had been chosen for another purpose. The devices were built by Texas Instruments under Rome Air Development Center contract # F30602-73-C-0027 for an application other than bandwidth reduction. Fortunately the tap weights had been chosen so as to approximately implement a cosine transform. Devices are being redesigned with the tap weights necessary for an exact odd cosine transform. The approximate cosine transform system has been constructed. The exact cosine transform system would have given a single pulse width of 10 microseconds for a line scan time of one millisecond and a sample rate of 100 samples per line. The approximate cosine system gives an output that is functionally like $\sin x/x$. The width and shape of the output agree with
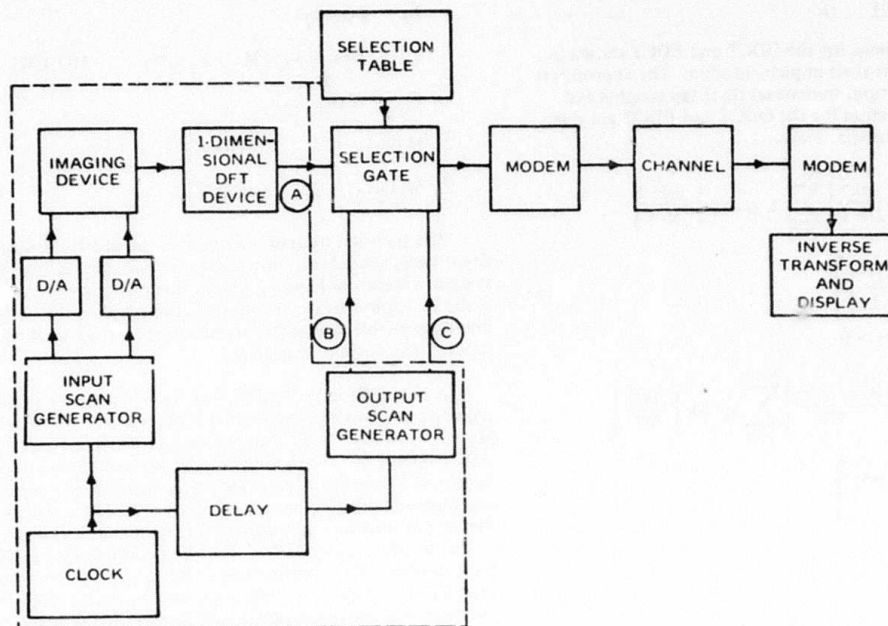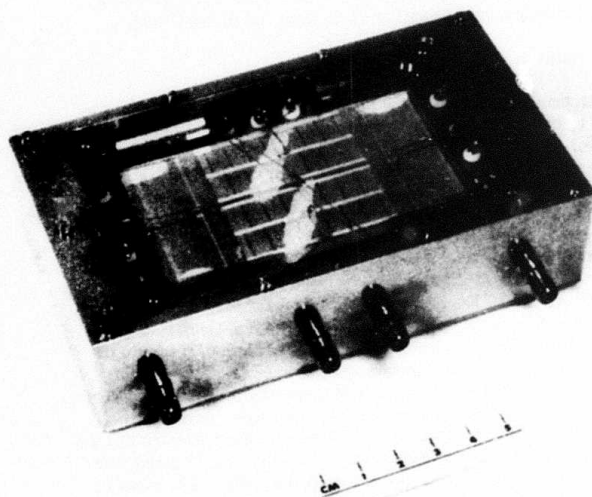
Fig. 7. *Reduced redundancy image transmission system using two-dimensional discrete Fourier transform device with linear congruential scan.*

CZT TRANSVERSAL FILTER

Fig. 8. SAW device.

computer simulation of the approximate cosine transform. This implies the filters and the multipliers are performing adequately.

Both the charge transfer device system and the surface acoustic wave system are light weight, low power, low cost systems that provide a capability of real-time bandwidth reduction.

SUMMARY

Several image transform coding systems have been described, analyzed, and tested by simulation. It has been shown that the two dimensional Cosine transform system and the hybrid Cosine transform/ DPCM system both provide significant bandwidth reduction with acceptable image quality and tolerance to channel errors. Implementation techniques particularly suited to these coding systems have been developed using acoustic surface wave delay lines and charge coupled devices for coding at real time television rates. Also, post processing techniques have been demonstrated for the reduction of quantization error in transform components.

REFERENCES

(1) P. A. Wintz. "Transform picture coding," IEEE Trans. Commun. Tech., Vol. COM-19, No. 6, pp. 809-820, December 1971.

(2) J. O. Limb, C. B. Rubinstein and K. A. Walsh, "Digital coding of color picturephone signals by element-differential quantization," IEEE Trans. Commun. Tech., Vol. COM-19, No. 6, pp. 992-1005, Dec. 1971.

(3) A. Habibi, "Comparison of nth-order DPCM encoder with linear transformations and block quantization techniques," IEEE Trans. Commun. Tech., Vol. COM-19, No. 6, pp. 948-956, Dec. 1971.

(4) W. K. Pratt, "Transform image coding spectrum extrapolation," Proceedings of Seventh Hawaii International Conference on Systems Sciences, pp. 7-9, January 1974.

(5) N. Ahmed, T. Natarajan and K. R. Rao, "Discrete Cosine transform," to appear in IEEE Trans. on Computers.

(6) Whitehouse, H. J., J. M. Speiser and R. W. Means, High Speed Serial Access Linear Transform Implementations, presented at the All Applications Digital Computer (AADC) Symposium, Orlando, Florida, 23-25 January 1973, reprinted in [9].

(7) H. E. Kallmann, "Transversal Filters," Proc. IRE, Vol. 28, pp. 302-310, July 1940.

(8) Preisendorfer, R. W., Introduction to Fast Fourier Transforms, Visibility Laboratory, University of California, San Diego, Spring 1967.

(9) Means, R. W., H. J. Whitehouse, et al, Image Transmission Via Spread Spectrum Techniques, ARPA Quarterly Technical Report March 1 – June 1, 1973. Order Number 2303, Code Number 3G10.

(10) Means, R. W., J. M. Speiser, H. J. Whitehouse, et al, Image Transmission Via Spread Spectrum Techniques, ARPA Quarterly Technical Report June 1 – October 1, 1973, Order Number 2303, Code Number 3G-10.

(11) Means, R. W., D. D. Buss, and H. J. Whitehouse, Real Time Discrete Fourier Transforms Using Charge Transfer Devices, Proceedings of the CCD Applications Conference held at the Naval Electronics Laboratory Center, San Diego, California, 18-20 Sept. 1973, pp. 95-101. Reprinted in [10].

(12) Alsup, J. M., R. W. Means, and H. J. Whitehouse, Real Time Discrete Fourier Transforms Using Surface Acoustic Wave Devices, to appear in the Proceedings of the IEEE International Specialist Seminar on Component Performance and Systems Applications of Surface Acoustic Wave Devices, held at Aviemore, Scotland, 24-28 Sept. 1973. Reprinted in [10].

APPENDIX B

HIGH SPEED SERIAL ACCESS IMPLEMENTATION
FOR DISCRETE COSINE TRANSFORMS

Jeffrey Speiser
Naval Undersea Center

INTRODUCTION

Two different types of discrete cosine transform (DCT) are useful for
reduced redundancy television image transmission [1-3]. Both are obtained by
extending the length N data block to have even symmetry, taking the discrete
Fourier transform (DFT) of the extended data block, and saving N terms of the
resulting DFT. Since the DFT of a real even sequence is a real even sequence,
either DCT is its own inverse if a normalized DFT is used.

The "Odd CDT" (ODCT) extends the length N data block to length 2N-1, with
the middle point of the extended block as a center of even symmetry. The
"Even DCT" (EDCT) extends the length N data block to length 2N, with a center
of even symmetry located between the two points nearest the middle. For
example, the odd length extension of the sequence A B C is C B A B C, and the
even length is C B A A B C. In both cases, the symmetrization eliminates the
jumps in the periodic extension of the data block which would occur if one
edge of the data block had a high value and the other edge had a low value;
in effect it performs a sort of smoothing operation with no loss of information.
It will be noted that the terms "odd" and "even" in ODCT and EDCT refer only to
the length of the extended data block - in both cases the extended data block
has even symmetry.

Both types of DCT may be implemented using compact, high speed, serial
access hardware, in structures similar to those previously described [1,2] for
the Chirp-Z transform (CZT) implementation of the DFT. The significant difference
between the ODCT and the EDCT is the block size of the transform which may be
implemented using transversal filters having a given limit on the number of
taps. A comparison of different high speed implementations of the DCT for a
block size of N is given in Table 1.

TYPE OF COSINE TRANSFORM	TYPE OF IMPLEMENTATION	FILTER LENGTH	# OF TIMES DATA POINTS ARE READ	# OF COMPLEX FILTERS NEEDED
ODCT	CZT OF LENGTH 2N-1 USING DEFINITION OF ODCT	4N-3	2	1
EDCT	CZT OF LENGTH 2N USING DEFINITION OF EDCT	4N-1	2	1
ODCT	FIRST N POINTS OF REAL PART OF CZT OF LENGTH 2N-1 OF N DATA POINTS FOLLOWED BY ZEROS	2N-1	1	1
EDCT	FIRST N POINTS OF REAL PART OF CZT OF LENGTH 2N OF N DATA POINTS	2N-1	1	1
EDCT	SWITCHING FILTER DCT	N	2	2

Table 1 - Comparison of Discrete Cosine Transform Implementations

ODD DISCRETE COSINE TRANSFORM

Let the data sequence be g_0, g_1, ..., g_{N-1}. The ODCT of g is defined as

$$G_{ok} = \sum_{j=-(N-1)}^{N-1} g_j \, e^{-\frac{i2\pi jk}{2N-1}} \qquad \text{for } k = 0, 1, \ldots, N-1 \tag{1}$$

where $g_{-j} = g_j$ for $j = 0, 1, \ldots, N-1$. $\tag{2}$

By straightforward substitution it may be shown that

$$G_{ok} = 2 \, \text{Re} \sum_{j=0}^{2N-2} \tilde{g}_j \, e^{-\frac{i2\pi jk}{2N-1}} \tag{3}$$

where $\tilde{g}_j$ is defined by equation (4).

$$\tilde{g}_j = \left\{ \begin{array}{l} .5 \, g_0, \; j = 0 \\ g_j, \; j = 1, \ldots, N-1 \\ 0, \; j = N, \ldots, 2N-2 \end{array} \right\} \tag{4}$$

The identity (5) may be used to obtain the CZT form of the ODCT shown in equation (6).

$$W^{jk} = W^{.5 k^2} \, W^{-.5(k-j)^2} \, W^{.5j^2} \tag{5}$$

$$G_{ok} = 2 \, \text{Re} \left\{ e^{-\frac{i\pi k^2}{2N-1}} \sum_{j=0}^{2N-2} \left[e^{-\frac{i\pi j^2}{2N-1}} \, \tilde{g}_j \right] e^{\frac{i\pi (k-j)^2}{2N-1}} \right\} \tag{6}$$

EVEN DISCRETE COSINE TRANSFORM

The EDCT of g is defined by equation (7), where the extended sequence is defined by equation (8).

$$G_{ek} = e^{-\frac{i\pi k}{2N}} \sum_{j=-N}^{N-1} g_j \, e^{-\frac{i2\pi jk}{2N}} \qquad \text{for } k = 0, 1, \ldots, N-1 \qquad (7)$$

$$g_{-1-j} = g_j \qquad \text{for } j = 0, 1, \ldots, N-1 \qquad (8)$$

If the mutually complex conjugate terms in equation (7) are combined, then equation (9) results. Equation (9) may be viewed as an alternate way of defining the EDCT.

$$G_{ek} = 2 \, \text{Re} \left\{ e^{-\frac{i\pi k}{2N}} \sum_{j=0}^{N-1} g_j \, e^{-\frac{i2\pi jk}{2N}} \right\} = 2 \sum_{j=0}^{N-1} g_j \cos\left[\frac{2\pi(j+.5)k}{2N}\right] \qquad (9)$$

Equation (9) may be put in either of the CZT formats given in equations (10) and (11), where $\tilde{\tilde{g}}_j$ is defined by equation (12).

$$G_{ek} = 2 \, \text{Re} \left\{ e^{-\frac{i\pi k}{2N}} \, e^{-\frac{i\pi k^2}{2N}} \sum_{j=0}^{N-1} \left[g_j \, e^{-\frac{i\pi j^2}{2N}} \right] e^{\frac{i\pi(k-j)^2}{2N}} \right\} \qquad (10)$$

$$G_{ek} = 2 \, \text{Re} \left\{ e^{-\frac{i\pi k}{2N}} \, e^{-\frac{i\pi k^2}{2N}} \sum_{j=0}^{2N-1} \left[\tilde{\tilde{g}}_j \, e^{-\frac{i\pi j^2}{2N}} \right] e^{\frac{i\pi(k-j)^2}{2N}} \right\} \qquad (11)$$

$$\tilde{\tilde{g}}_j = \left\{ \begin{array}{l} g_j, \; j = 0, 1, \ldots, N-1 \\ 0, \; j = N, \ldots, 2N-1 \end{array} \right\} \qquad (12)$$

IMPLEMENTATION OF THE DCT VIA THE CZT

A general DFT of length M, defined by equation (13) may be computed by a CZT defined by equations (15) and (16) as shown in Figure 1.

$$H_k = \sum_{j=0}^{M-1} h_j \; e^{-\frac{i2\pi jk}{M}} \tag{13}$$

$$H_k = P_k^* \sum_{j=0}^{M-1} [h_j \; P_j^*] \; P_{k-j} \tag{14}$$
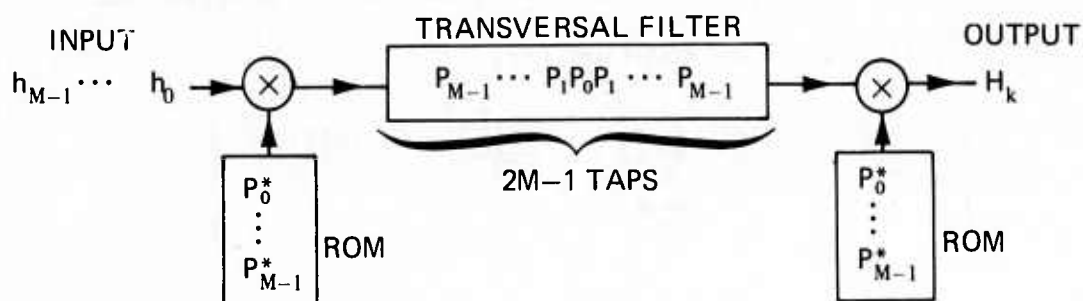
$$P_s = e^{\frac{i\pi s^2}{M}} = P_{-s} \tag{15}$$

Figure 1 - General DFT Implemented via a CZT
Using a Transversal Filter.

It will be noted that the postmultiplier of Figure 1 is ready to produce the first transform point when the first input to the filter is lined up with the central tap.

If the ODCT is viewed as a DFT using equation (1), then it may be implemented using the structure shown in Figure 1 with M = 2N-1, and the required filter length is 2M-1 which equals 4N-3.

The EDCT as defined by equation (7) may be implemented similarly with M = 2N by changing the postmultiplier weights to $e^{\frac{-i\pi(k^2+k)}{2N}}$.

R. Means has noted that a twofold reduction in the required length of the filter and read only memories is possible [4] when the ODCT is computed via equation (3) with a CZT used to perform the required DFT. Since only N terms of the input are non-zero, and only N terms of the transversal filter's output are needed, only the first N outputs of the ROMs and the central 2N-1 taps of the transversal filter of Figure 1 are needed when the ODCT is computed this way. A similar conclusion holds for the EDCT computed via equation (9) with a CZT used to compute the required DFT.

IMPLEMENTATION OF THE EDCT USING SWITCHING FILTERS

The computationally difficult step in the realization of the EDCT via equation (10) is the convolution-like operation shown in equation (16).

$$A_k = \sum_{j=0}^{N-1} a_j \, e^{\frac{i\pi(j-k)^2}{2N}} \qquad \text{for } k = 0, 1, \ldots, N-1 \qquad (16)$$

If P_s is defined by equation (15) with $M = 2N$, the convolution-like character of equation (16) may be made more explicit as shown in equation (17).

$$A_k = \sum_{j=0}^{N-1} a_j \, P_{j-k} = \sum_{j=0}^{N-1} a_j \, P_{k-j} \qquad (17)$$

Equation (17) would represent a (periodic) convolution or correlation if the P sequence had period N. In our case, however, the P sequence has period 2N. The essential symmetries of the P sequence are given by equations (18) and (19).

$$P_s = P_{-s} \qquad (18)$$

$$P_{N-s} = e^{\frac{i\pi(N^2 - 2Ns + s^2)}{2N}} = (-1)^s \, e^{\frac{i\pi N}{2}} \, P_s \qquad (19)$$

For specific values of N, equation (19) can be simplified further by using equation (20).

$$e^{\frac{i\pi N}{2}} = \begin{cases} 1, & N = 0 \ (\text{mod } 4) \\ i, & N = 1 \ (\text{mod } 4) \\ -1, & N = 2 \ (\text{mod } 4) \\ -i, & N = 3 \ (\text{mod } 4) \end{cases} \qquad (20)$$

Table 2 shows the weights needed to evaluate (17), where identity (18) has been used to eliminate negative indices. Table 3 shows the same weights after additional simplification using identities (19) and (20) when N is a multiple of four,to view the weights needed at successive times as modifications of cyclic shifts of P_0, P_1, . . ., P_{N-1}. Table 4 shows the weights of Table 3 arranged to correspond to cyclic shifts of the data, corresponding to an implementation using length N transversal filters with data points read twice.

SHIFT INDEX	WEIGHT SET						
0	P_{N-1} · · ·					P_1	P_0
1	P_{N-2} · · ·				P_1	P_0	P_1
2	P_{N-3} · · ·			P_2	P_0	P_1	P_2
.							
.							
.							
N-1	P_0	P_1	P_2 · · ·			P_1	P_{N-1}

Table 2 - Weights Required for the Correlation-Like Operation
in the IDCT, Ordered for Fixed Data Position.

SHIFT INDEX	WEIGHT SET					
0	P_{N-1} $\cdots$				P_1	P_0
1	P_{N-2} $\cdots$			P_1	P_0	$-P_{N-1}$
2	P_{N-3} $\cdots$		P_1	P_0	$-P_{N-1}$	P_{N-2}
3	P_{N-4} $\cdots$	P_1	P_0	$-P_{N-1}$	P_{N-2}	$-P_{N-3}$
·						
·						
·						
k	$P_{N-k-1} \cdots P_1$ $P_0 \cdots \pm \cdots$				$(-1)^{k-1}P_{N-k+1}$	$(-1)^k P_{N-k}$

Table 3 - Reduced Form of the Weights Required for the Correlation-Like Operation in the EDCT when $N = 0$ (Mod 4), Ordered for Fixed Data Position.

SHIFT INDEX	WEIGHT SET			
0	P_{N-1} $\cdots$		P_1	P_0
1	$-P_{N-1}$	P_{N-2}	P_1	P_0
2	$-P_{N-1}$	P_{N-2} $P_{N-3} \cdots$	P_1	P_0
3	$-P_{N-1}$	P_{N-2} $-P_{N-3} \cdots$	P_1	P_0

Table 4 - Weights Required for the Correlation-Like Operation in the EDCT when $N = 0$ (Mod 4) Ordered for Cyclically Shifting Data.

The required time-variant operations may be moved out of the filters as shown in Figure 2.
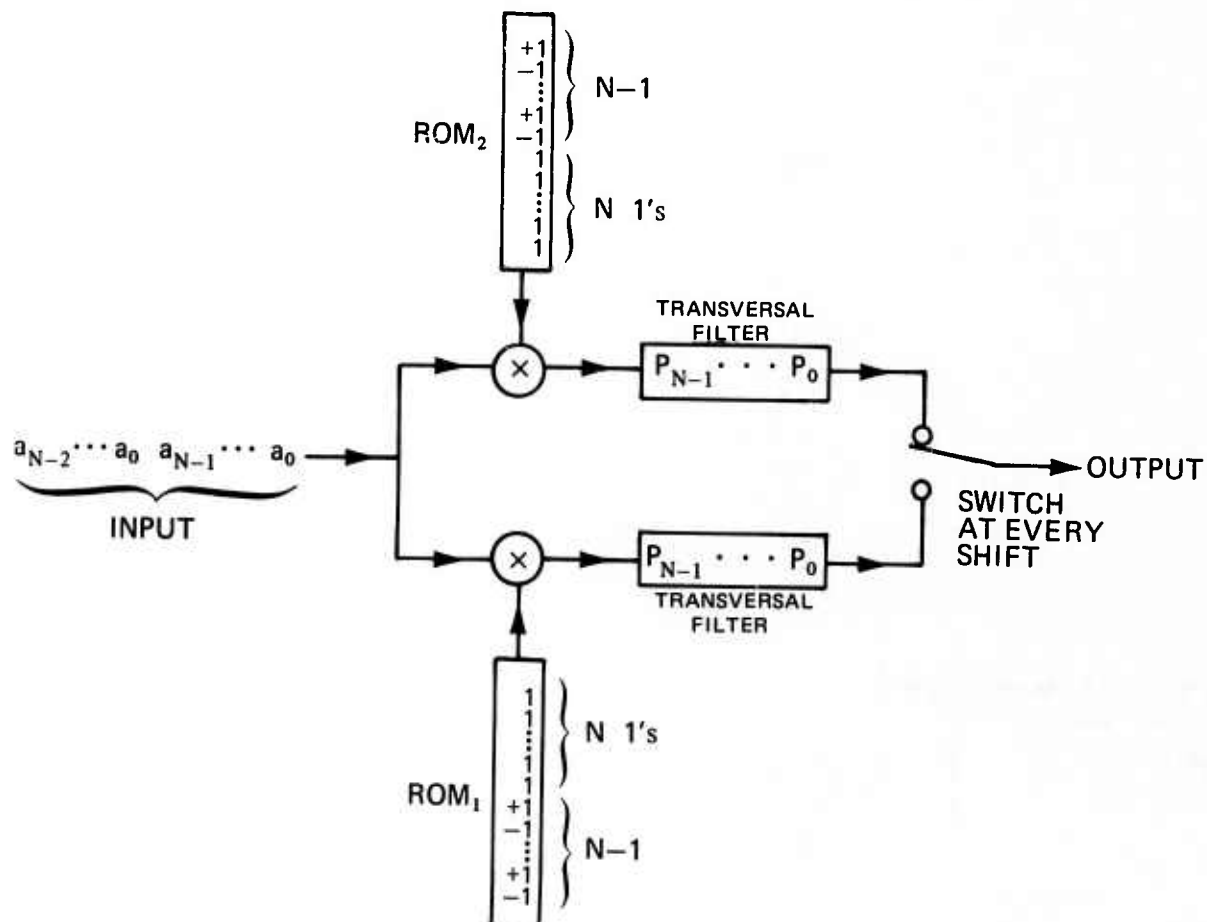

Figure 2 - Switching Filter for use in the EDCT for
$N = 0(\text{Mod } 4)$ or $N = 2(\text{Mod } 4)$

A complete EDCT structure using the switching filter is shown in Figure 3. The switch changes position with every data shift, and its initial position is determined by whether the block size is congruent to zero or two modulo four. A similar structure may be used for block sizes congruent to one or three modulo four, except that ROM 1 and ROM 2 will contain ± i entries instead of

± l's. Because of the simple structure of the output needed from ROM 1 and
ROM 2 it may be preferable to replace them with a combination of a counter and
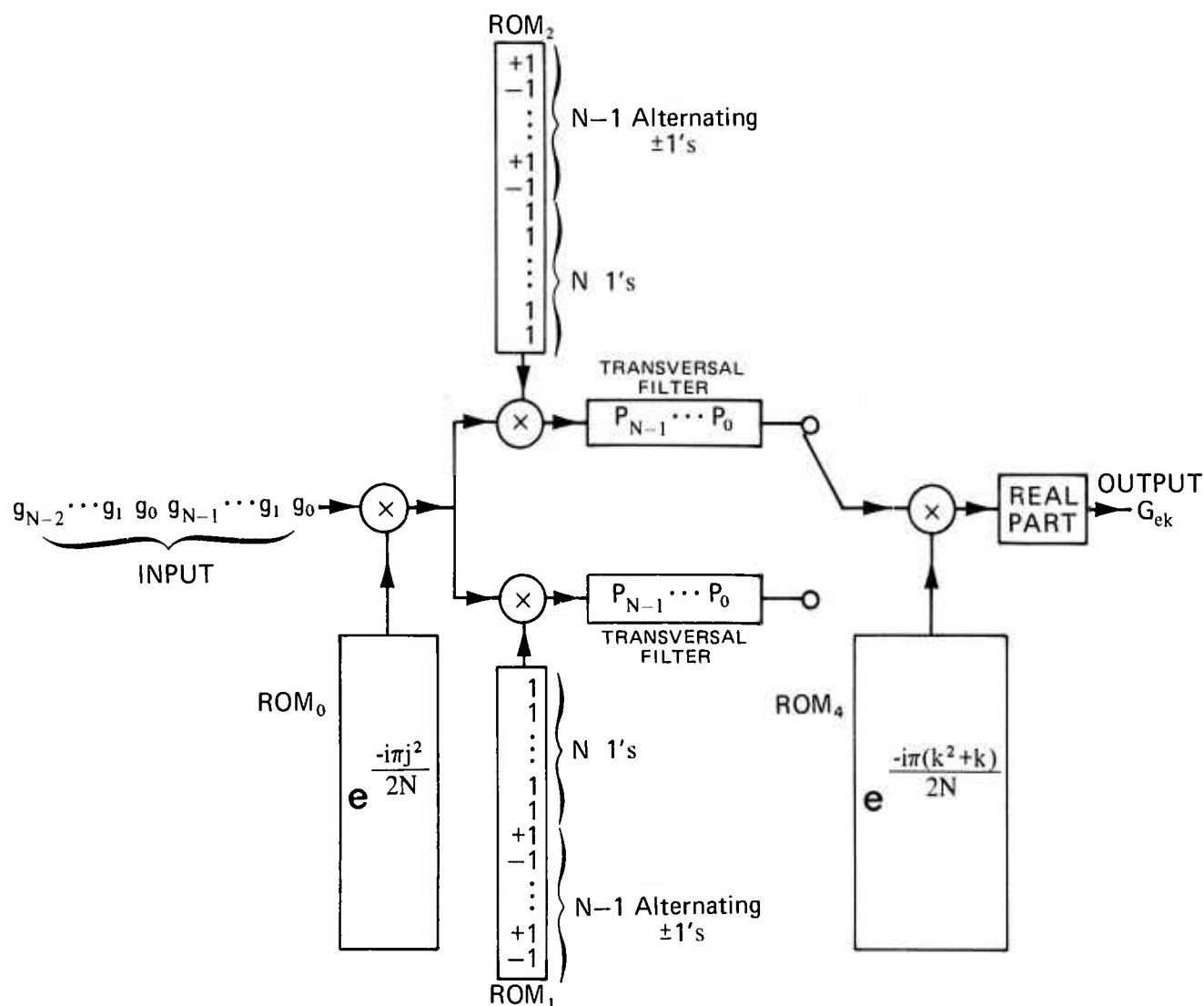gates to generate the required functions.

Figure 3 - EDCT Architecture using Switching Filter

CONCLUSIONS

The three general types of DCT implementations using transversal filters
and multipliers each possess unique advantages. A DCT implementation using a
complete CZT will use transversal filters with tap weightings which should
become standard components in the near future. An implementation using
shortened versions of the filters and ROMs needed for a standard CZT permits a
longer block length transform to be implemented for a given number of taps per
filter, and simultaneously eliminates the need to rescan data points. A new
structure called the "switching filter EDCT" permits a further increase in
block size for a given filter length, but requires more filters, some additional
switching circuitry, and a rescan of the data. The switching filter implemen-
tation of the EDCT uses transversal filters each having a number of taps equal
to the transform block length. The other implementations require nearly twice
as many and four times as many taps per filter.

ACKNOWLEDGEMENT

REFERENCES

1. Means, R. W., H. J. Whitehouse, et al, Image Transmission Via Spread Spectrum Techniques, ARPA Quarterly Technical Report, March 1 - June 1, 1973, Order Number 2303, Code Number 3G10.

2. Means, R. W., J. M. Speiser, H. J. Whitehouse, et al, Image Transmission Via Spread Spectrum Techniques, ARPA Quarterly Technical Report, June 1 - October 1, 1973, Order Number 2303, Code Number 3G10.

3. Ahmed, N., T. Natarajan, and K. R. Rao, On Image Processing and a Discrete Cosine Transform, to appear in the IEEE Transactions on Electronic Computers.

4. Means, R. W., private communication.

APPENDIX C

TWO-DIMENSIONAL DISCRETE COSINE TRANSFORM
IMPLEMENTATION USING A TOROIDAL SCAN

Jeffrey Speiser
Naval Undersea Center

INTRODUCTION

Two different types of one-dimensional discrete cosine transform (DCT) called the Even DCT (EDCT) and Odd DCT (ODCT) which are useful for reduced redundancy image transmission [1-3] may be combined to form three distinct types of two-dimensional discrete cosine transform. Each of the two-dimensional DCTs may be defined as a two-dimensional discrete Fourier transform (DFT) of a doubly symmetrized extension of the data block in which the extended data block has even symmetry about each of two axes. If the original data block size was N_1 by N_2, the extended block size may be $2N_1$ by $2N_2$ for the EDCT by EDCT, $2N_1-1$ by $2N_2$ for the ODCT by EDCT, or $2N_1-1$ by $2N_2-1$ for the ODCT by ODCT.

Although the three types of two-dimensional DCT may be expected to provide similar performance for television image redundancy reduction, they differ markedly with respect to difficulty of real-time implementation. Each of the two transforms may, of course, be implemented by performing a line-by-line one-dimensional partial transform, using an auxiliary "corner-turning" memory to store and transpose the partial transform, and then perform a partial transform in the second dimension.

It has previously been shown that a two-dimensional DFT may be implemented as a one-dimensional DFT of size $M = M_1M_2$ of an appropriate linear congruential scan of an M_1 by M_2 data block, provided that M_1 and M_2 have no common divisor [1]. Since $2N_1$ and $2N_2$ have the common divisor of 2, the linear congruential scan does not aid in performing a two-dimensional EDCT. For a two-dimensional ODCT, the linear congruential scan will be compatible with certain block sizes, but never when the block is square. For a hybrid ODCT by EDCT two-dimensional transform, the linear congruential scan is compatible with all square block sizes, since 2N and 2N-1 never have a common divisor.

It will be shown that the linear congruential scan converts a hybrid ODCT by EDCT of an N by N data block into a length $N(2N-1)$ one-dimensional EDCT which may be implemented via a switching filter EDCT [4] using transversal filters of length $N(2N-1)$. For a given upper limit on the number of taps in the transversal filter, the hybrid ODCT by EDCT therefore permits a larger block size than would be possible with a two-dimensional ODCT, and a vastly simpler implementation than would be needed for a two-dimensional EDCT. A comparison of the two-dimensional DCT implementations for an N_1 by N_2 block size is given in Table 1.

Table 1 - Comparison of Two-Dimensional Discrete Cosine Transform
Implementations Using Linear Congruential Scans.

TYPE OF TRANSFORM	TYPE OF IMPLEMENTATION	FILTER LENGTH	NUMBER OF TIMES DATA POINTS ARE READ	NUMBER OF COMPLEX FILTERS NEEDED
ODCT by ODCT	linear congruential scan to convert to one-dimensional ODCT, implemented by real part of truncated filter CZT	$(2N_1-1)$ $(2N_2-1)$	2	1
ODCT by EDCT	linear congruential scan to convert to one-dimensional EDCT, implemented by real part of truncated filter CZT	$(2N_1-1)$ $(2N_2)-1$	2	1
ODCT by EDCT	linear congruential scan to convert to one-dimensional EDCT, implemented by switching filter EDCT	$N_2(2N_1-1)$	4	2

C-4

SYMMETRIES PRESERVED BY SELECTED TOROIDAL SCANS

For a two-dimensional DFT to be equivalent to a one-dimensional DFT, the two-dimensional block size M_1 by M_2 must be such that M_1 and M_2 have no common divisor. In that case, the two-dimensional DFT of equation (1) will be equivalent to the one-dimensional DFT of equation (2) with $M = M_1 M_2$. The appropriate linear congruential input scan is defined by equations (3) and (4), and the associated output scan is defined by equations (5) and (6). The constants u_1, v_1, u_2, v_2 may be any solution of equations (7) and (8).

$$G_{(k_1,k_2)} = \sum_{j_1=0}^{M_1-1} \sum_{j_2=0}^{M_2-1} g_{(j_1,j_2)} \, e^{-i2\pi\left[\frac{j_1 k_1}{M_1} + \frac{j_2 k_2}{M_2}\right]} \tag{1}$$

$$\text{for } k_1 = 0, \ldots, M_1-1$$
$$k_2 = 0, \ldots, M_2-1$$

$$F_q = \sum_{p=0}^{M-1} f_p e^{\frac{-i2\pi pq}{M}} \qquad \text{for } q = 0, \ldots, M-1 \tag{2}$$

$$p(j_1,j_2) = j_1 u_1 M_2 + j_2 u_2 M_1 \qquad (\text{MOD } M) \tag{3}$$

$$f_p = g(j_1,j_2) \tag{4}$$

$$q(k_1,k_2) = k_1 v_1 M_2 + k_2 v_2 M_1 \qquad (\text{MOD } M) \tag{5}$$

$$F_q = G(k_1,k_2) \tag{6}$$

$$M_2 u_1 v_1 = 1 \qquad (\text{MOD } M_1) \tag{7}$$

$$M_1 u_2 v_2 = 1 \qquad (\text{MOD } M_2) \tag{8}$$

The behavior of the input scan is extremely simple to describe if v_1 and v_2 are both chosen equal to one. In this case, to move from the presently scanned point to the next point, each coordinate is incremented by 1, and the first coordinate is reduced modulo M_1 and the second coordinate is reduced modulo M_2, as shown in equation (9). The notation $(a)_b$ denotes the residue of a modulo b. Such a scan may be viewed as a spiral on the surface of a torus. The required scan generator is simply a pair of counters and digital to analog converters.

$$p\left((s+1)_{M_1},\ (s+1)_{M_2}\right) \ = \ p\left((s)_{M_1},(s)_{M_2}\right) + 1 \qquad \text{(Modulo M)} \qquad (9)$$

Equation (9) will now be proved. From (7) and (8) it follows that $(M_2 u_1 - 1)$ is a multiple of M_1 and $(M_1 u_2 - 1)$ is a multiple of M_2. The product is therefore a multiple of $M_1 M_2$ as shown in equation (10).

$$(M_2 u_1 - 1)\ (M_1 u_2 - 1) \ = \ 0 \qquad \text{(Modulo M)} \qquad (10)$$

Simplification of (10) yields (11).

$$p(1,1) \ = \ M_2 u_1 + M_1 u_2 \ = \ 1 \qquad \text{(Modulo M)} \qquad (11)$$

Equation (12) follows from the scan defining equation (3).

$$p\left((s+1)_{M_1},(s+1)_{M_2}\right) = (s+1)u_1 M_2 + (s+1)u_2 M_1 = p\left((s)_{M_1},(s)_{M_2}\right) + p(1,1) \qquad (12)$$

The desired equation (9) follows from (11) and (12). Since the scan takes the two-dimensional origin (0,0) into the one-dimensional origin 0, equation (9) may be solved by induction to yield the closed form scan equation (13).

$$p\left((s)_{M_1},\ (s)_{M_2}\right) \ = \ s \qquad \text{(Modulo M)} \qquad (13)$$

Equation (13) says that the kth coordinate of the point scanned at time s is obtained by reducing s modulo M_k.

The scanning of a data block which has been symmetrized for the two-dimensional ODCT will now be considered in detail. The data block is extended using the double mirror symmetry defined in equation (14).

$$g(\pm j_1, \pm j_2) = g(j_1, j_2) \tag{14}$$

The two-dimensional DFT of the extended data block defines the two-dimensional DCT of the original data block given in equation (15), with $M_k = 2N_k - 1$.

$$G(k_1, k_2) = \sum_{j_1 = -(N_1-1)}^{N_1-1} \sum_{j_2 = -(N_2-1)}^{N_2-1} g(j_1, j_2) \, e^{-i2\pi\left[\frac{j_1 k_1}{M_1} + \frac{j_2 k_2}{M_2}\right]} \tag{15}$$

Since the indices are only defined modulo M_1 and M_2 respectively, the summation limits in (15) are really no different from those in (1). If the scan is defined by equations (3) and (4), then the symmetry of the corresponding one-dimensional sequence is shown in equation (16).

$$f_{-p} = g(-j_1, -j_2) = g(j_1, j_2) = f_p \tag{16}$$

The toroidal scan of the extended data block - which is, of course, obtained by repeatedly scanning points of the original data block - is illustrated in Table 2 for a block size of 2 by 3. The numbers in the table indicate the scan order, while the letters indicate the data values.

Table 2A - Toroidal Scan for an ODCT of a 2 by 3 Data Block

```
    F        E        F
   -7        3       -2

    D        C        D
   -1       -6        4
   ┌ ─ ─ ─ ─ ─ ─ ─ ┐
    B    │   A        B
    5    │   0       -5
                             ⎫
    D    │   C        D      ⎬  N₂ = 3
   -4    │   6        1      ⎭

    F    │   E        F
    2    │  -3        7
   └ ─ ─ ─ ─ ─ ─ ─ ┘
        ⎵⎵⎵⎵⎵⎵
         N₁ = 2
```

$N_2 = 3$

$N_1 = 2$

Table 2B - One-Dimensional Sequence Produced by a Toroidal Scan
for an ODCT of a 2 by 3 Data Block.

INDEX	DATA VALUE
-7	F
-6	C
-5	B
-4	D
-3	E
-2	F
-1	D
0	A
1	D
2	F
3	E
4	D
5	B
6	C
7	F

The symmetry of a sequence produced by a toroidal scan of a data block symmetrized for a hybrid ODCT by EDCT will now be examined. The symmetrization for the hybrid two-dimensional ODCT by EDCT is described by the requirement that each pair of points of the extended data block, $(j_1 j_2)$ and (j_1^*, j_2^*) have the same data value whenever the points satisfy equation (17).

$$j_1 = j_1^* \quad \text{or} \quad j_1 + j_1^* = 0 \qquad \text{(Modulo } M_1) \qquad (17A)$$

$$j_2 = j_2^* \quad \text{or} \quad j_2 + j_2^* = -1 \qquad \text{(Modulo } M_2) \qquad (17B)$$

Equations (18) and (19) examine the point scanned k samples after (N_1, N_2) and k samples before the previous point (N_1-1, N_2-1).

$$p(N_1, N_2) + k = p\left((N_1+k)_{M_1}, (N_2+k)_{M_2}\right) \qquad \text{(Modulo } M) \qquad (18)$$

$$p(N_1-1, N_2-1) - k = p\left((N_1-1-k)_{M_1}, (N_2-1-k)_{M_2}\right) \qquad \text{(Modulo } M) \qquad (19)$$

The sum of the first coordinates for the points on the right-hand side of equations (18) and (19) is given in equation (20). The corresponding sum for the second coordinates is given in equation (21).

$$(N_1+k) + (N_1-1-k) = 2N_1-1 = 0 \qquad \text{(Modulo } M_1) \qquad (20)$$

$$(N_2+k) + (N_2-1-k) = 2N_2-1 = -1 \qquad \text{(Modulo } M_2) \qquad (21)$$

It therefore follows from equation (17) that the two points have the same data value as shown in equation (22).

$$f\left(p(N_1, N_2) + k\right) = f\left(p(N_1-1, N_2-1) - k\right) \qquad (22)$$

C-9

If the toroidal scan is therefore used, starting at point (N_1, N_2) of the extended image, the resulting sequence will have the symmetry required for a one-dimensional EDCT. The toroidal scan of a 2 by 2 data block extended for the two-dimensional hybrid ODCT by EDCT is shown in Table 3.

Table 3A - Toroidal Scan of a 2 by 2 Data Block Examined for the Two-Dimensional Hybrid ODCT by EDCT.

D	C	C	D
2	11	8	5
B	A	A	B
6	3	0	9
D	C	C	D
10	7	4	1

$$\left. \right\} \; N_1 = 2$$

$$\underbrace{\qquad} \; N_2 = 2$$

Table 3B - One-Dimensional Sequence Produced by the Toroidal Scan of a 2 by 2 Data Block Symmetrized for a Two-Dimensional Hybrid ODCT by EDCT.

INDEX	DATA VALUE
8	C
9	B
10	D
11	C
0	A
1	D
2	D
3	A
4	C
5	D
6	B
7	C

LINEAR CONGRUENTIAL SCAN GENERATORS FOR SYMMETRIZED DATA BLOCKS

A toroidal scan of an actual M_1 by M_2 data block was shown by equation (9) to be obtained by successively adding 1 to each of the scan coordinates and reducing the sums modulo M_1 and M_2, respectively.

The corresponding results when the data block is a symmetric extension of an N_1 by N_2 data block are shown in Table 4. Note that the kth scan has period M_k as a function of the one-dimensional scan index, so that only M_k successive values for the kth scan need be shown. It will be noted that, unlike the case of the linear congruential scan for the two-dimensional DFT, each scan coordinate changes by at most one from one scanned point to the next.

Table 4A - Scanning Function for the kth Coordinate
of a Two-Dimensional DCT Symmetrized to Odd
Length on the kth Coordinate

INDEX	j_k (MODULO M_k)	j_k REDUCED TO ORIGINAL DATA BLOCK
0	0	0
1	1	1
.	.	.
.	.	.
.	.	.
N_k-1	N_k-1	N_k-1
N_k	$-(N_k-1)$	N_k-1
.	.	.
.	.	.
.	.	.
$2N_k-2$	-1	1

Table 4B - Scanning Function for the kth Coordinate
of a Two-Dimensional DCT Symmetrized to Even Length
on the kth Coordinate. $(M_k = 2N_k)$

INDEX	j_k (MODULO M_k)	j_k REDUCED TO ORIGINAL DATA BLOCK
0	0	0
1	1	1
.	.	.
.	.	.
.	.	.
N_k-1	N_k-1	N_k-1
N_k	N_k	N_k-1
.	.	.
.	.	.
.	.	.
$2N_k-2$	-2	1
$2N_k-1$	-1	0

The vertical and horizontal scan functions may be thought of as sampled triangular waveforms. During a complete sampling of the extended data block, M_2 complete periods of the triangular waveform of period M_1 occur, and M_1 complete periods of the triangular waveform of period M_2 occur.

An analog version of the required scan may be obtained by sampling the integral of a square wave. A digital version may be obtained from an up-down counter with appropriate gating to reverse the count direction when necessary.

CONCLUSIONS

It has been shown that two different types of two-dimensional DCT may be implemented as one-dimensional DCTs of an appropriate scan of the data block. For a hybrid ODCT by ODCT, a single complex filter of length $(2N_1-1)(2N_2-1)$ is needed. For a hybrid ODCT by EDCT, either two complex filters of length $N_2(2N_1-1)$ or a single complex filter of length $(2N_1-1)(2N_2)-1$ is needed. The required scan on each coordinate is a sampled triangular wave and thus may be easily generated and has no abrupt changes of the coordinate values.

REFERENCES

[1] Means, R. W., H. J. Whitehouse, et al, Image Transmission via Spread
Spectrum Techniques, ARPA Quarterly Technical Report, March 1 - June 1,
1973, Order Number 2303, Code Number 3G10.

[2] Means, R. W., J. M. Speiser, H. J. Whitehouse, et al, Image Transmission
Via Spread Spectrum Techniques, ARPA Quarterly Technical Report, June 1 -
October 1, 1973, Order Number 2303, Code Number 3G10.

[3] Ahmed, N., T. Natarajan, and K. R. Rao, On Image Processing and a Discrete
Cosine Transform, to appear in the IEEE Transactions on Electronic
Computers.

[4] Speiser, J. M., High Speed Serial Access Implementation for Discrete
Cosine Transforms, NUC TN 1265, 8 January 1974.

APPENDIX D

ON THE EQUIVALENCE OF ONE- AND TWO-DIMENSIONAL FOURIER TRANSFORMS

James W. Bond
Naval Undersea Center

ON THE EQUIVALENCE OF ONE AND TWO DIMENSIONAL FOURIER TRANSFORMS

By J. W. Bond

ABSTRACT

Two dimensional discrete Fourier transforms can be calculated by ordering an N_1 by N_2 array of data and calculating a one-dimensional Fourier transform, provided N_1 and N_2 are relatively prime. This note shows how any isomorphism from the direct sum of the integers modulo N_1 and N_2 to the integers modulo $N_1 N_2$ can be used to relate one and two dimensional discrete Fourier Transforms. Among the available isomorphisms it is always possible to choose one that has either a particularly simple input scan or a particularly simple output scan. Both the input and output scans can be particularly simple only when N_1 and N_2 differ by one. These simple scans consist of spiraling along a discrete torus. Such scans can be calculated with a pair of counters modulo the horizontal and vertical block size.

INTRODUCTION

Discrete Fourier transforms have been of considerable interest since the discovery of algorithms, known as Fast Fourier Transforms, which enable the rapid calculation of discrete Fourier transforms on digital computers. R. W. Preisendorfer[**] noticed that one-dimensional Fourier transforms of length N could be implemented as two dimensional N_1 by N_2 Fourier transforms when $N_1 N_2 = N$ with N_1 and N_2 relatively prime and an isomorphism of the integers modulo N is used onto the direct sum of the integers module N_1 and the integers module N_2.

Jeff Speiser and Harper Whitehouse realized that such an isomorphism could also be used to implement the two-dimensional discrete Fourier transform as a one-dimensional transform. They suggested a particular architecture which would enable the calculation of two-dimensional Fourier transforms at much higher rates than the FFT implementations which are usually used at present.[*] In this report it is shown that either the input scan or output scan utilized in this architecture can be chosen as a simple diagonal scan on the torus.

---

[*]*R. W. Means, Speiser, J. M., Whitehouse, H. J., et. al, Image Transmission via Spread Spectrum Techniques, ARPA Quarterly Technical Report June 1 – October 1, 1973, Order Number 2303 Code Number 3G10.*

[**]*R. W. Preisendorfer, Introduction to Fast Fourier Transforms, Visibility Lab, University of California, San Diego, Spring 1967.*

Furthermore, it is shown that both input and output scans can be chosen to be simple only when the array block sizes differ by one.

THE DIAGONAL SCAN

An N_1 by N_2 scan is defined by specifying an N_1 by N_2 matrix $S = (n_{ij})$, where $\{n_{ij}\}$ is $\{n \mid o \leqslant n \leqslant N_1 N_2 - 1\}$. The result of a scan applied to an N_1 by N_2 array of data $A = (a_{ij})$ is to order the data corresponding to n_{ij}. For example, the scan $\begin{pmatrix} 0 & 4 & 2 \\ 3 & 1 & 5 \end{pmatrix}$ applied to the data $\begin{pmatrix} a & b & c \\ d & e & f \end{pmatrix}$ orders the data a, e, c, d, b, f.

The simplest scan of interest in this note begins with 0 in the upper lefthand corner and numbers successively down the diagonal according to the rules shown in Figure 1. Figure 2 contains examples which indicate that the diagonal scan covers an N_1 by N_2 array if and only if N_1 and N_2 are relatively prime. This result is established in Corollary 1 of Proposition 1.

DISCRETE FOURIER TRANSFORMS AND DIAGONAL SCANS

Suppose throughout this section that N_1 and N_2 are relatively prime. The top corner of the diagonal scan of an N_1 by N_2 array has the form

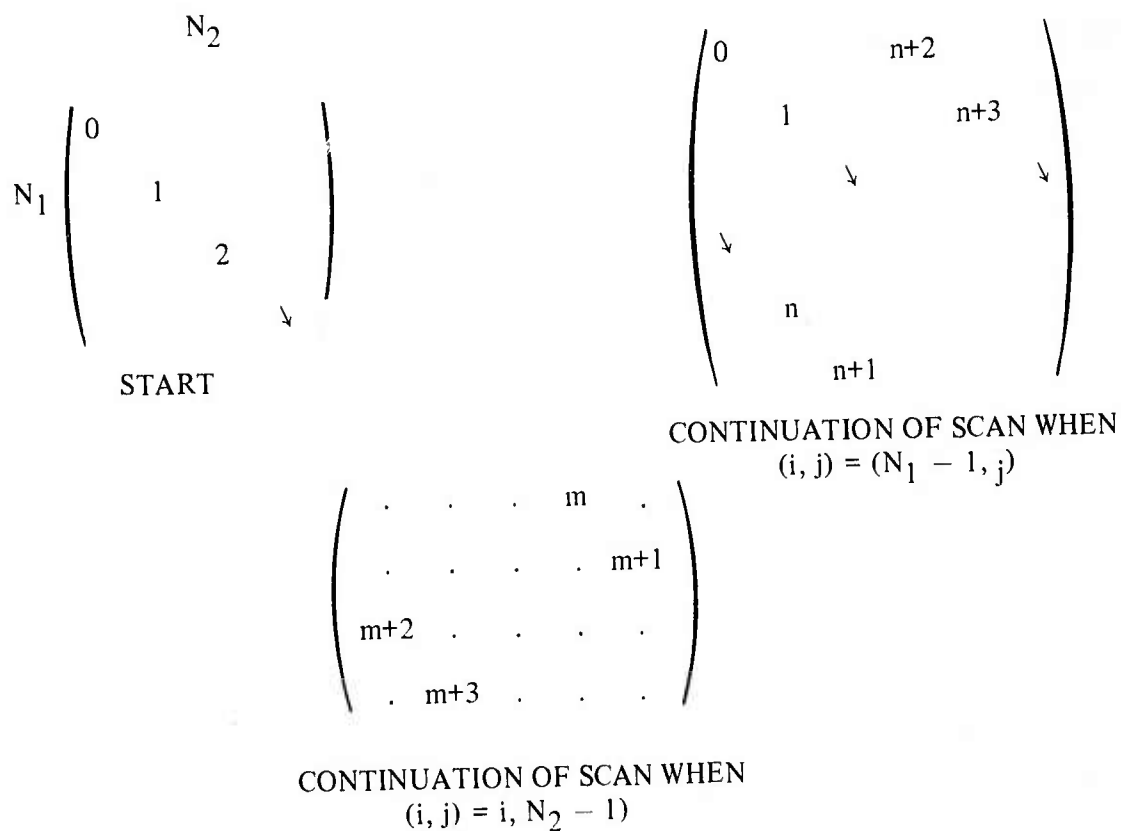$$\begin{pmatrix} 0 & u_2 N_1 \\ u_1 N_2 & 1 \end{pmatrix}$$

Later we will show that the integer in the j_1, j_2 spot of the diagonal scan is the integer between 0 and $N_1 N_2 - 1$ congruent modulo $N_1 N_2$ to $j_1 u_1 N_2 + j_2 u_2 N_1$, u_1, u_2 integers.

Given real or complex numbers $o \leqslant j_1 \leqslant N_1 - 1$, $o \leqslant j_2 \leqslant N_2 - 1$, let

$$f_p = g_{(j_1, j_2)}, \text{ where } p \equiv (j_1 u_1 N_2 + j_2 u_2 N_1) \text{ modulo } N_1 N_2. \text{ Then if}$$

$$F_q = \sum_{p=o}^{N_1 N_2 - 1} f_p \exp(-i 2\pi pq / N_1 N_2), \text{ the sequence}$$

$F_o, F_1, \ldots, F_{N_1 N_2 - 1}$ is called the discrete Fourier transform (D F T) of the sequence $f_o, f_1, \ldots, f_{N_1 N_2 - 1}$.

N_2

N_1 $\begin{pmatrix} 0 & & & \\ & 1 & & \\ & & 2 & \\ & & & \searrow \end{pmatrix}$

START

$\begin{pmatrix} 0 & & n+2 & \\ & 1 & & n+3 \\ & & \searrow & & \searrow \\ \searrow & & & & \\ n & & & \\ & n+1 & & \end{pmatrix}$

CONTINUATION OF SCAN WHEN
$(i, j) = (N_1 - 1, j)$

$\begin{pmatrix} . & . & . & m & . \\ & . & . & . & . & m+1 \\ m+2 & . & . & . & . \\ & . & m+3 & . & . & . \end{pmatrix}$

CONTINUATION OF SCAN WHEN
$(i, j) = i, N_2 - 1)$

Inductive definition of scan

Assign 0 to (0,0). If n has been assigned to (i, j) then $n + 1$ is assigned to $(i + 1, j + 1)$ with $i + 1$ reduced to zero when $i = N_1 - 1$ and with $j + 1$ reduced to zero when $j = N_2 - 1$ provided an integer has not already been assigned to $(i + 1, j + 1)$. Note the indices run from 0 to $N_1 - 1$ or $N_2 - 1$ rather than from 1 to N_1 or N_2.

Note also that if k is assigned to (i, j) then i is the least nonnegative integer congruent to k modulo N_1 and j is the least nonnegative integer congruent k modulo N_2.

Figure 1. Definition of the Diagonal Scan.

$$N_1 = 3 \quad N_2 = 5 \qquad\qquad N_1 = 2 \quad N_2 = 4$$

$$\begin{pmatrix} 0 & 6 & 12 & 3 & 9 \\ 10 & 1 & 7 & 13 & 4 \\ 5 & 11 & 2 & 8 & 14 \end{pmatrix} \qquad \begin{pmatrix} 0 & & 2 & \\ & 1 & & 3 \end{pmatrix}$$

$$N_1 = 4 \quad N_2 = 5 \qquad\qquad N_1 = 4 \quad N_2 = 6$$

$$\begin{pmatrix} 0 & 16 & 12 & 8 & 4 \\ 5 & 1 & 17 & 13 & 9 \\ 10 & 6 & 2 & 18 & 14 \\ 15 & 11 & 7 & 3 & 19 \end{pmatrix} \qquad \begin{pmatrix} 0 & & 8 & & 4 & \\ & 1 & & 9 & & 5 \\ 6 & & 2 & & 10 & \\ & 7 & & 3 & & 11 \end{pmatrix}$$

$$N_1 = 4 \quad N_2 = 7 \qquad\qquad N_1 = 3 \quad N_2 = 6$$

$$\begin{pmatrix} 0 & 8 & 16 & 24 & 4 & 12 & 20 \\ 21 & 1 & 9 & 17 & 25 & 5 & 13 \\ 14 & 22 & 2 & 10 & 18 & 26 & 6 \\ 7 & 15 & 23 & 3 & 11 & 19 & 27 \end{pmatrix} \qquad \begin{pmatrix} 0 & & & 3 & & \\ & 1 & & & 4 & \\ & & 2 & & & 5 \end{pmatrix}$$

Note The diagonal scan exhausts an N_1 by N_2 array if and only if N_1 and N_2 are relatively prime. Indeed the diagonal scan naturally defines an isomorphism from the direct sum of integers modulo N_1 and N_2 to the integers modulo the least common multiple of N_1 and N_2.

Figure 2. Examples of the Diagonal Scan.

Let

$$q = k_1 N_2 + k_2 N_1, \quad k_1, k_2 \text{ integers,}$$

then

$$F_{k_1 N_2 + k_2 N_1}$$

$$= \sum_{j_1=0}^{N_1-1} \sum_{j_2=0}^{N_2-1} f_{j_1 u_1 N_2 + j_2 u_2 N_1} \exp\left((-i\, 2\pi/N_1 N_2)\, (j_1 u_1 N_2 + j_2 u_2 N_1)\,(k_1 N_2 + k_2 N_1)\right)$$

since $\exp(-i\, 2\pi/N_1 N_2)\, N_1 N_2 = 1$, the exponents can be reduced modulo $N_1 N_2$.

Since the diagonal scan has 1 assigned to (1,1) we have $u_1 N_2 + u_2 N_1 \equiv 1 \bmod N_1 N_2$.

Conclude from multiplication by N_2 from this equation that $u_1 N_2^2 \equiv N_2 \bmod N_1 N_2$ and by N_1 that $u_2 N_1^2 \equiv N_1 \bmod N_1 N_2$. Thus

$$(j_1 u_1 N_2 + j_2 u_2 N_1)\,(k_1 N_2 + k_2 N_1) \equiv j_1 k_1 u_1 N_2^2 + j_2 k_2 u_2 N_1^2$$

$$\equiv (j_1 k_1 N_2 + j_2 k_2 N_1) \bmod N_1 N_2.$$

Therefore

$$F_{k_1 N_2 + k_2 N_1}$$

$$= \sum_{j_1=0}^{N_1-1} \sum_{j_2=0}^{N_2-1} (f_{j_1 u_1 N_2 + j_2 u_2 N_1}) \exp\left((-i\, 2\pi/N_1 N_2)\, (j_1 k_1 N_2 + j_2 k_2 N_1)\right)$$

and the n

$$G_{(0,\,0)} = F_0, \ldots, G_{(k_1,\, k_2)} = F_{k_1 N_2 + k_2 N_1} \cdots$$

is the two-dimensional DFT of $g_{(0,\,0)}, \ldots, g_{(k_1,\, k_2)}, \ldots, g_{(N_1 - 1,\, N_2 - 1)}$.

To see this simply note that the previous equation when written in terms of $g_{(j_1,j_2)}$ and $G_{(k_1,k_2)}$ is

$$G_{(k_1,k_2)} = \sum_{j_1=0}^{N_1-1} \sum_{j_2=0}^{N_2-1} g_{(j_1,j_2)} \exp[-i\, 2\pi\, (j_1 k_1/N_1 + j_2 k_2/N_2)] \ .$$

The output scan associated with mapping $(k_1, k_2) \rightarrow (k_1 N_2 + k_2 N_1)$ is described in Figure 3. Examples of input diagonal scans and output scans are illustrated in Figure 4; the output scan appears to be simple when N_1 and N_2 differ by 1. That this is the only case when the output scan is simple is discussed in the concluding paragraphs of this report. Note that the output scan can be viewed as proceeding on diagonals perpendicular to the input scan when N_1 and N_2 differ by one.

THE GENERAL THEORY

Let Z_N denote the additive group of residue classes modulo N. An element of Z_N consists of all integers that differ by a multiple of N.

The direct sum of two groups Z_{N_1} and Z_{N_2} is the group written $Z_{N_1} + Z_{N_2}$ consisting of pairs of elements one from Z_{N_1} and one from Z_{N_2} with component addition.

The group $Z_{N_1} + Z_{N_2}$ and $Z_{N_1 N_2}$ are isomorphic (i.e., structurally the same) if and only if N_1 and N_2 are relatively prime. The clearest way to see this is to exhibit a generic homomorphism from $Z_{N_1} + Z_{N_2}$ into $Z_{N_1 N_2}$ and show that some of the homomorphisms are onto if and only if N_1 and N_2 are relatively prime.

Any homomorphism ψ of $Z_{N_1} + Z_{N_2}$ into $Z_{N_1 N_2}$ is completely determined by $\psi(1,0)$ and $\psi(0,1)$ for $\psi(j_1,j_2) = j_1 \psi(1,0) + j_2 \psi(0,1)$. Furthermore $N_1 \psi(1,0) = \psi(N_1,0) = \psi(0,0) = 0$ and $N_2 \psi(0,1) = \psi(0,N_2) = \psi(0,0) = 0$ because any homomorphism must take $(0,0)$ onto 0. If we interpret the residue classes $\psi(1,0)$ and $\psi(0,1)$ as integers between 0 and $N_1 N_2 - 1$, then $N_1 \psi(1,0)$ and $N_2 \psi(0,1)$ must be divisible by $N_1 N_2$ so that $\psi(1,0) = u_1 N_2$ and $\psi(0,1) = u_2 N_1$ for some integers u_1 and u_2 between, respectively, 0 and $N_1 - 1$ and 0 and $N_2 - 1$. Therefore $\psi(j_1,j_2) = j_1 u_1 N_2 + j_2 u_2 N_1$ for $0 \leqslant j_1 \leqslant N_1 - 1$, $0 \leqslant j_2 \leqslant N_2 - 1$. The term ψ will be onto when the $j_1 u_1 N_2 + j_2 u_2 N_1$ reduce Modulo $N_1 N_2$ to all the integers between 0 and $N_1 N_2 - 1$.

D-7

If the input scan is the diagonal scan

$$\begin{pmatrix} 0 & u_2N_1 & & & \\ u_1N_2 & 1 & & & \\ & & 2 & & \\ & & & \ddots & \\ & & & & \ddots \end{pmatrix}$$

then the output scan is

$$\begin{pmatrix} 0 & N_1 & & & \\ N_2 & N_1+N_2 & & & \\ & & 2(N_1+N_2) & & \\ & & & \ddots & \\ & & & & \ddots \end{pmatrix}$$

Figure 3. The Output Scan Associated with an Input Diagonal Scan.

Consider the set $S = \{j_1u_1N_2 + j_2u_2N_1, j_1, j_2 \text{ integers}\}$ and let d be the least positive element of S. It is easy to show that d is the greatest common divisor of u_1N_2, u_2N_1.

Suppose that $d = ia+jb$ is the least positive integer in $\{ia + jb \mid i, j \text{ integers}\}$ and d did not divide a. Then $a = kd + r$ with $0 < r < d$ (the division algorithm). So $r = a - kd = a - k(ia + jb) = a(1 - ki) + (-j)b$, which is an element of S, contradicting the choice of d. Likewise d divides b. Next if d' divides both a and b then it divides every sum $ia + jb$, hence it divides d. Therefore d is the greatest common divisor of a and b.

INPUT   OUTPUT

$$N_1 = 5 \quad N_2 = 7$$

$$\begin{pmatrix} 0 & 15 & 30 & 10 & 25 & 5 & 20 \\ 21 & 1 & 16 & 31 & 11 & 26 & 6 \\ 7 & 22 & 2 & 17 & 32 & 12 & 27 \\ 28 & 8 & 23 & 3 & 18 & 33 & 13 \\ 14 & 29 & 9 & 24 & 4 & 19 & 34 \end{pmatrix} \quad \begin{pmatrix} 0 & 5 & 10 & 15 & 20 & 25 & 30 \\ 7 & 12 & 17 & 22 & 27 & 32 & 2 \\ 14 & 19 & 24 & 29 & 34 & 4 & 9 \\ 21 & 26 & 31 & 1 & 6 & 11 & 16 \\ 28 & 33 & 3 & 8 & 13 & 18 & 23 \end{pmatrix}$$

$$N_1 = 5 \quad N_2 = 6$$

$$\begin{pmatrix} 0 & 25 & 20 & 15 & 10 & 5 \\ 6 & 1 & 26 & 21 & 16 & 11 \\ 12 & 7 & 2 & 27 & 22 & 17 \\ 18 & 13 & 8 & 3 & 28 & 33 \\ 24 & 19 & 11 & 9 & 4 & 29 \end{pmatrix} \quad \begin{pmatrix} 0 & 5 & 10 & 15 & 20 & 25 \\ 6 & 11 & 16 & 21 & 26 & 1 \\ 12 & 17 & 22 & 27 & 2 & 7 \\ 18 & 23 & 28 & 3 & 8 & 13 \\ 24 & 29 & 4 & 9 & 14 & 19 \end{pmatrix}$$

Figure 4. Examples of Input Diagonal Scans and Associated Output Scans

If we reduce the elements of S modulo $N_1 N_2$ we will get all integers between 0 and $N_1 N_2 - 1$ if and only if there exists e such that $de \equiv 1 \bmod N_1 N_2$, i.e., d is a unit in the residue class modulo $N_1 N_2$. This is immediate when we observe all the elements in S are of the form kd, k an integer. If $kd \equiv 1 \bmod N_1 N_2$ for some k, then every integer can be obtained between 0 and $N_1 N_2 - 1$; conversely, if 1 is not of this form, then 1 is not in the image.

PROPOSITION 1

Let $\psi : Z_{N_1 + N_2} \rightarrow Z_{N_1 N_2}$ be a homomorphism.
Then ψ has the form:

$\psi(j_1, j_1) = j_1 u_1 N_2 + j_2 u_2 N_1$ with the common divisor of $u_1 N_2$ and $u_2 N_1$ in the integers is a unit in the intergers modulo $N_1 N_2$.

Proof

We have shown that any homomorphism has the above form, but we have not shown that ψ is well defined, i.e., if $j_1 - j'_1 = kN_1$ and $j_2 - j'_2 = k'N_2$ then $\psi(j_1,j_2) - \psi(j'_1,j'_2) = k'' N_1 N_2$. But, $\psi(j_1,j_2) - \psi(j'_1,j'_2) = j_1 u_1 N_2 + j_2 u_2 N_1 - (j'_1 u_1 N_2 + j'_2 u_2 N_1)$
$= (j_1 - j'_1) u_1 N_2 + (j_2 - j'_2) u_2 N_1 = kN_1 u_1 N_2 + k'N_2 u_2 N_1 = (ku_1 + k'u_2) N_1 N_2$.

Corollary 1

$Z_{N_1} + Z_{N_2}$ is isomorphic to $Z_{N_1 N_2}$ if and only if N_1 and N_2 are relatively prime.

Proof

If $d > 1$ divides N_1 and N_2 then $dk \equiv 0 \bmod N_1 N_2$ with $0 < k < N_1 N_2 - 1$. Note then that if $dk' \equiv 1 \bmod N_1 N_2$ for some k'', $dk' - 1 = k'' N_1 N_2$ and hence $dkk' - k = kk'' N_1 N_2$, i.e., $k''N_1 N_2 - k = k\,k'' N_1 N_2$ or $k \equiv 0 \bmod N_1 N_2$, a contradiction.

Now we wish to work out the relationship between scans and homomorphisms. Suppose ψ is a homomorphism from $Z_{N_1} + Z_{N_2}$ into $Z_{N_1 N_2}$.

Then

$$
\begin{pmatrix}
\psi(0,0) & \psi(0,1) & \ldots & \psi(0,N_2-1) \\
\psi(1,0) & \psi(1.1) & \ldots & \psi(1,N_2-1) \\
\vdots & \vdots & & \vdots \\
\psi(N_1-1,0) & \psi(N_1-1,1) & \ldots & \psi(N_1-1,N_2-1)
\end{pmatrix}
$$

is the associated scan.

PROPOSITION 2

The diagonal scan defines a homomorphism from Z_L onto $Z_{N_1} + Z_{N_2}$ where L is the least common multiple of N_1 and N_2.

Proof

Note by the definition of the diagonal scan of an N_1 by N_2 array shown in Figure 1 every element of the first row is divisible by N_1 and every element of the first column is divisible by N_2. The assignment of integers continues until the bottom corner is reached so

that the next spot is zero. Then if we let L–1 denote the entry in the bottom corner L must be congruent to 0 for the scan to define a homomorphism. Since L is congruent to an element in the first row and first column it is a common multiple of N_1 and N_2. Therefore $L \geq$ the least common multiple of N_1 and N_2.

Next consider what pairs (j_1, j_2) can be assigned integers by a diagonal scan. Let d be the greatest common divisor of N_1 and N_2. Note that the integers reached come from (k, k) with k reduced modulo N_1 in the first index and k reduced modulo N_2 in the second index. Therefore if (j_1, j_2) is assigned an integer, we have $(j_1, j_2) = (k+k_1 N_1, k+k_2 N_2)$ for some integers k_1 and k_2; so that $j_1 - j_2 = k_1 N_1 - k_2 N_2 = k_3$ d. In particular, the only integers reached in the first row (i.e., when $j_1 = 0$) are multiples of d and in the first column are multiples of d. More generally, the diagonal only fills out 1/d of the array. Therefore at most 1/d of the locations in an array can be covered by the scan. Since $N_1 N_2/d$ is the least common multiple of N_1 and N_2, we have $L \leq$ the least common multiple of N_1 and N_2. Thus L is the least common multiple of N_1 and N_2.

Next, we work out the relationship between discrete Fourier transforms and the isomorphisms we have been constructing. It will turn out that the mappings under discussion must be isomorphisms.

If ψ is any one to one mapping of $Z_{N_1} + Z_{N_2}$ onto $Z_{N_1 N_2}$ then it induces a mapping ψ^* from the functions indexed by $Z_{N_1 N_2}$ to those indexed by $Z_{N_1} + Z_{N_2}$ by defining $(\psi^* f)_{(k_1, k_2)} = f_{\psi(k_1, k_2)}$.

Let DFT^1 denote the one dimensional Fourier transform which maps a function indexed by Z_L into functions indexed by Z_L. In particular

$$F_q = DFT_q^1 (f) = \sum_{p=0}^{L-1} f_p \exp ((-i\, 2\pi/L)\, pq).$$

Let DFT^2 denote the two dimensional Fourier transform which maps a function g indexed by $Z_{N_1} + Z_{N_2}$ into a function indexed by $Z_{N_1} + Z_{N_2}$. In particular, $G(k_1, k_2) = DFT^2_{(k_1, k_2)}(g)$

$$= \sum_{j_1=0}^{N_1-1} \sum_{j_2=0}^{N_2-1} g_{(j_1 j_2)} \exp\left[-i\,2\pi\,(j_1 k_1/N_1 + j_2 k_2/N_2)\right]$$

$$= \sum_{j_1=0}^{N_1-1} \sum_{j_2=0}^{N_2-1} g_{(j_1 j_2)} \exp\left((-i\,2\pi/N_1 N_2)(k_1 j_1 N_2 + k_2 j_2 N_1)\right)$$

The relationship between DFT^1 and DFT^2 is summarized in the following proposition.

PROPOSITION 3

a) If ψ and φ are on-to-one maps from $Z_{N_1} + Z_{N_2}$ onto $Z_{N_1 N_2}$ such that the diagram

commutes then;

   1) N_1 and N_2 are relatively prime and

   2) ψ and φ are isomorphisms of $Z_{N_1} + Z_{N_2}$ onto $Z_{N_1 N_2}$.

   b) If ψ is any isomorphism of $Z_{N_1} + Z_{N_2}$ onto $Z_{N_1 N_2}$ then there exists an isomorphism φ so that the diagram

commutes.

D-12

c) If $\psi(j_1, j_2) = j_1 u_1 N_2 + j_2 u_2 N_1$ then

$\varphi(k_1, k_2) = k_1 v_1 N_2 + k_2 v_2 N_1$ with $u_1 v_1 N_2 + u_2 v_2 N_1 = 1$.

Note that the commutativity of the above diagrams is simply the mathematical way to say that by utilizing the maps ψ^* and φ^* either DFT^2 can be implemented by DFT^1, namely, $G = \varphi^* \{DFT^1 [\psi^{*-1} (g)]\}$, or DFT^1 can be implemented by DFT^2, namely $F = \varphi^{*-1} \{DFT^2 [\psi^* (f)]\}$. Proposition 3 shows that these implementations are only possible when N_1 and N_2 are relatively prime and the mappings of indices are isomorphisms of the group of residue classes under addition.

Before proving the proposition we prove the following Lemmas.

Lemma 1

If

then $\quad \psi(j_1, j_2) \varphi(k_1 k_2) \equiv j_1 k_1 N_2 + j_2 k_2 N_1 \mod N_1 N_2$.

Proof

That the diagram commutes means that

$G = DFT^2 (\psi^* f) = \varphi [DFT^1 (f)]$

To calculate $DFT^2 (\psi^* f) = \varphi [DFT^1 (f)]$ consider the component mapping

$DFT^2 (k_1, k_2) = G_{(k_1, k_2)}$

$$= \sum_{j_1=0}^{N_1-1} \sum_{j_2=0}^{N_2-1} (\psi^* f)_{(j_1, j_2)} \exp (i \, 2\pi/N_1 N_2) (j_1 k_1 N_2 + j_2 k_2 N_1)$$

$$= \sum_{j_1=0}^{N_1-1} \sum_{j_2=0}^{N_2-1} f_{\psi(j_1, j_2)} \exp (-i \, 2\pi/N_1 N_2) (j_1 k_1 N_2 + j_2 k_2 N_1)$$

D-13

To calculate $\varphi \, [\text{DFT}^1 \, (f)]$ let $G = \varphi^* \, F$. Then

$$G_{(k_1, k_2)} = F_{\varphi(k_1, k_2)} = \sum_{p=0}^{N_1 N_2 - 1} f_k \exp(-i \, 2\pi/N_1 N_2) \, \varphi \, (k_1, k_2) \, p$$

$$= \sum_{j_1=0}^{N_1-1} \sum_{j_2=0}^{N_2-1} f_{\psi(j_1, j_2)} \exp(-i \, 2\pi/N_1 N_2) \, \varphi \, (k_1, k_2) \, \psi \, (j_1, j_2) \, .$$

The two expressions are the same only if $\varphi \, (k_1, k_2) \, \psi \, (j_1, j_2) \equiv j_1 k_1 N_2 + j_2 k_2 N_1 \bmod N_1 N_2$ for all j_1, j_2, k_1, k_2.

Lemma 2

If $\psi \, (j_1, j_2) \, \varphi \, (k_1, k_2) \equiv (j_1 k_1 N_2 + j_2 k_2 N_1) \bmod N_1 N_2$ for all integers j_1, j_2, k_1, k_2 then ψ and φ one to one mappings of $Z_{N_1} + Z_{N_2}$ onto $Z_{N_1 N_2}$ implies that ψ and φ are isomorphisms.

Proof

For (j'_1, j'_2) such that $\psi \, (j'_1, j'_2) = 1$, $\varphi \, (k_1 + k'_1, k_2 + k'_2) \equiv j'_1 \, (k_1 + k'_1) \, N_2 + j'_2 \, (k_2 + k'_2) \, N_1 \equiv (j'_1 k_1 N_2 + j'_2 k_2 N_1) + (j'_1 k'_1 N_2 + j'_2 k'_2 N_1) \equiv \varphi \, (k_1, k_2) + \varphi \, (k'_1, jk'_2) \bmod N_1 N_2$.

Likewise for $\varphi \, (k'_1 \, k'_2)$ such that $\varphi \, (k'_1, k'_2) = 1$ it follows that ψ is a homomorphism.

Lemmas 1 and 2 complete the proof of part (a) of proposition 3. To prove b, note that if $\psi \, (j_1, j_2) = j_1 u_1 N_2 + j_2 u_2 N_1$, then the existence of φ is equivalent to the existence of v_1 and v_2 such that $\varphi \, (k_1, k_2) = k_1 v_1 N_2 + k_2 v_2 N_1$ and

$$(j_1 u_1 N_2 + j_2 u_2 N_1) \, (k_1 v_1 N_2 + k_2 v_2 N_1) \equiv (j_1 k_1 N_2 + j_2 k_1 N_1) \bmod N_1 N_2 \, .$$

Let v_1 and v_2 satisfy $u_1 v_1 N_2 + u_2 v_2 N_1 \equiv 1 \bmod N_1 N_2$ which also has a solution since $u_1 N_2$ and $u_2 N_1$ have greatest common divisor in the integers which is a unit in $Z_{N_1 N_2}$. If v'_1 and v'_2 solves $u_1 v'_1 N_2 + u_2 v'_2 N_1 = d$, d the greatest common divisor of $u_1 N_2$ and $u_2 N_1$, then $v_1 \equiv e \, v'_1 \bmod N_1 N_2$ and $v_2 \equiv e \, v'_2 \bmod N_1 N_2$ where $de \equiv 1 \bmod N_1 N_2$ will provide a solution to $u_1 v_1 N_2 + u_2 v_2 N_1 \equiv 1 \bmod N_1 N_2$.

From $u_1v_1N_2 + u_2v_2N_1 \equiv 1 \bmod N_1N_2$ it follows from multiplication by N_1 and N_2 that $u_2v_2N_1{}^2 \equiv N_1 \bmod N_1N_2$ and $u_1v_1N_2{}^2 \equiv N_2 \bmod N_1N_2$. These congruences allow us to calculate modulo N_1N_2

$$(j_1u_1N_2 + j_2u_2N_1)(k_1v_1N_2 + k_2v_2N_1) \equiv j_1k_1u_1v_1N_2{}^2 + j_2k_2u_2v_2N_1{}^2$$

$$\equiv j_1k_1N_2 + j_2k_2N_1 ,$$

which completes the proof of proposition 3.

There are two natural symmetries in the scans associated with an isomorphism. These arise because

$$\psi(j_1 + 1, j_2 + 1) - \psi(j_1, j_2) = u_1N_2 + u_2N_1$$

and

$$\psi(j_1 + 1, j_2 - 1) - \psi(j_1, j_2) = u_1N_2 - u_2N_1$$

are independent of (j_1, j_2).

The simplest possible scans occur when one of these two differences is one.

Note that if $\psi(j_1 + 1, j_2 + 1) - \psi(j_1, j_2) = 1$ then $v_1 = 1$, $v_2 = 1$ and $\varphi(k_1, k_2)$ $= k_1N_2 + k_2N_1$ defines the output scan so that the output scan is only simple when N_1 and N_2 differ by one since $\psi(j_1 + 1, j_2 - 1) - \psi(j_1, j_2) = \pm 1$. This results because for all cases of interest $N_1 + N_2$ is small composed with N_1N_2. $u_1N_2 - u_2N = 1$ then $v_1 = 1$ $v_2 = -1$ provides a solution and $\varphi(j_1, j_2) = j_1N_2 - j_2N_1$, and here the only time that $\psi(j_1 + 1, j_2 + 1) - \psi(j_1, j_2) = \pm 1$ is when N_1 and N_2 differ by one. Therefore, the input and output scans are simple only when N_1 and N_2 are both relatively prime and differ by one.

From $u_1 v_1 N_2 + u_2 v_2 N_1 \equiv 1 \bmod N_1 N_2$ it follows from multiplication by N_1 and N_2 that $u_2 v_2 N_1{}^2 \equiv N_1 \bmod N_1 N_2$ and $u_1 v_1 N_2{}^2 \equiv N_2 \bmod N_1 N_2$. These congruences allow us to calculate modulo $N_1 N_2$

$$(j_1 u_1 N_2 + j_2 u_2 N_1)(k_1 v_1 N_2 + k_2 v_2 N_1) \equiv j_1 k_1 u_1 v_1 N_2{}^2 + j_2 k_2 u_2 v_2 N_1{}^2$$

$$\equiv j_1 k_1 N_2 + j_2 k_2 N_1 ,$$

which completes the proof of proposition 3.

There are two natural symmetries in the scans associated with an isomorphism. These arise because

$$\psi(j_1 + 1, j_2 + 1) - \psi(j_1, j_2) = u_1 N_2 + u_2 N_1$$

and

$$\psi(j_1 + 1, j_2 - 1) - \psi(j_1, j_2) = u_1 N_2 - u_2 N_1$$

are independent of (j_1, j_2).

The simplest possible scans occur when one of these two differences is one.

Note that if $\psi(j_1 + 1, j_2 + 1) - \psi(j_1, j_2) = 1$ then $v_1 = 1$, $v_2 = 1$ and $\varphi(k_1, k_2) = k_1 N_2 + k_2 N_1$ defines the output scan so that the output scan is only simple when N_1 and N_2 differ by one since $\psi(j_1 + 1, j_2 - 1) - \psi(j_1, j_2) = \pm 1$. This results because for all cases of interest $N_1 + N_2$ is small composed with $N_1 N_2$. $u_1 N_2 - u_2 N = 1$ then $v_1 = 1$ $v_2 = -1$ provides a solution and $\varphi(j_1, j_2) = j_1 N_2 - j_2 N_1$, and here the only time that $\psi(j_1 + 1, j_2 + 1) - \psi(j_1, j_2) = \pm 1$ is when N_1 and N_2 differ by one. Therefore, the input and output scans are simple only when N_1 and N_2 are both relatively prime and differ by one.

APPENDIX E

A SIGNAL PROCESSING SENSOR USING CCDs

H. J. Whitehouse
I. Lagnado

ABSTRACT

A new signal processing sensor is possible using a combination of charge transfer devices and signal processing concepts which simultaneously measures the incident optical signal and performs a linear transformation upon that signal. This paper will discuss possible implementations and the types of transforms which may be performed. It appears possible, at this time, to perform the Discrete Fourier Transform in a linear imaging device. Extension of the concept to a two-dimensional array may be feasible.

INTRODUCTION

In signal processing optical images often constitute one of the many forms which signals may take. These images are typically processed either optically by means of moving transparencies or optical diffraction cells through which the image passes prior to its detection by a photodetector, or the optical signals are converted to electrical signals by means of image sensors and these electrical signals are subsequently processed electronically.

In this paper a new optical sensor is proposed which combines the functions of signal processor and image sensor in a single photosensitive silicon Charge Coupled Device (CCD). For simplicity of description and ease of fabrication a one dimensional signal processing sensor is described. However, in many of its applications a two dimensional array of one dimensional sensors would be required. In principle, these two dimensional arrays can be formed by the juxtaposition of a number of one dimensional arrays on a single silicon chip with common clocks to all CCD registers.

ARCHITECTURE

Both 500 X 1 and 100 X 100 photosensitive silicon CCD arrays have been commercially fabricated[1] using buried channel techniques with small charge transfer inefficiencies at clock rates in excess of 1 MHz. Using similar techniques, it appears feasible to simultaneously control the amount of photogenerated charge and its transverse transfer to the CCD shift registers. Successive iteration of the charge generation and transfer corresponds to a weighted superposition of lagged versions of the image and thus corresponds to a discrete convolution of the image as sampled by the spatial structure of the sensor with the time function represented by the transfer signal. Thus, in a single structure, are combined the functions of image sensing, spatial to temporal multiplexing, and convolution. A block diagram of a signal processing array is shown in Fig. 1. The discrete nature of the CCD image sensor is indicated by the boxes indicated by "array", the controlled transfer of the generated charge is indicated by "multiplication", and the CCD registers are indicated by "delay". The serial output of the signal processing array thus occurs at the clock rate of the CCD registers which may not be regular.

1. Fairchild Camera & Instrument Corp.; Syosset, New York.

Since convolution and correlation are both basic to signal processing, their interpretation as discrete spatial operations will be reviewed. The cross convolution and correlation of two continuous functions are given by equations (1) and (2) respectively:

(a) convolution $\quad [f \star g] (x) = \int_{-\infty}^{\infty} f(\eta)\, g(x-\eta)\, d\eta \qquad\qquad$ (1)

(b) correlation $\quad [f \otimes g] (x) = \int_{-\infty}^{\infty} f(\eta)\, g(x+\eta)\, d\eta \qquad\qquad$ (2)

The corresponding relationships for discrete functions may be found by replacing the integrals by products as given in equations (3) and (4):

(a) convolution $\quad [f \star g]_n = \sum_k f_n\, g_{n-k} \qquad\qquad$ (3)

(b) correlation $\quad [f \otimes g]_n = \sum_k f_n\, g_{n+k} \qquad\qquad$ (4)

The value of the discrete convolution or correlation may be viewed as the coefficient of Z^n in the polynomial products 3′ and 4′ respectively.

Thus

$$\sum_n (f \star g)_n\, Z^n = \left(\sum_e f_e\, Z^e\right)\left(\sum_m g_m\, Z^m\right) \qquad\qquad (3')$$

and

$$\sum_n (f \otimes g)_n\, Z^n = \left(\sum_e f_e Z^{-e}\right)\left(\sum_m g_m\, Z^m\right) \qquad\qquad (4')$$

As an example the convolution and correlation of the binary sequence $1,1,\overline{1},1,$ with a non negative sequence $1,1,1,1$ is given below where overbar denotes negation.

(a) convolution   1,2,1,2,1,0,1

(b) correlation   1,0,1,2,1,2,1

Due to the representation of the sampled variable by the amount of minority charge in the potential well induced in the silicon, only numbers of a fixed sign can be represented. This presents a problem when it is desired to convolve the data with a sequence having both positive and negative terms. This difficulty does not arise in ordinary image sensors since simple sensing of the light intensity requires only numbers of the same sign. Unfortunately, the solution which is used in signal processing applications of CCD of adding a fixed bias of half the maximum value of the input signal is difficult for a signal processing image sensor, since the bias signal would then need to be optical at half the intensity of the maximum optical input. However, by designing an image sensor with two CCD registers and bidirectional charge transfer, it is possible to sense the difference between the charge in the two registers, and in this way, represent both positive and negative numbers.

Two applications of this proposed signal processing image sensor are considered as examples of its potential use. These are real time cross correlation or filtering, and transform image encoding. Cross-correlation uses spatially-uniform time-varying illumination. Transform image encoding uses a spatially-varying illumination which is constant during this processing interval.

An optical cross correlator or optical filter is shown diagrammatically in Fig. 2. The input signal f modulates the light output from a photo diode one focal distance in front of a converging lens. The collimated light then falls on the signal processing image sensor whose transfer gates are controlled by the signal g. The output from the sensor will then be the cross correlation of the input signal f with the transfer gate signal g, and will be available in real time at the same clock rate as the input signal f. This is an improvement proportional to $\log_2 N$ in the rate of computation over evaluation by "in place" digital computation using the "fast convolution" algorithm on a computer with the same cycle time as the input signal sample rate.

A transform image encoder is shown diagrammatically in Fig. 3. An input object is at infinity before a converging lens of focal length d. An image is formed a distance d behind

the lens on a signal processing image sensor. If a signal g is applied to the transfer gates of the Signal Processing Image Sensor (SPIS), the cross correlation of the image and the signal g will be obtained as an output, provided the image is stationary for the duration of the signal f.

Proposed Solution

The signal processing concepts presented and illustrated above may be implemented by an idealized structure shown in Fig. 4. The suggested device configuration will allow the controlled routing and algebraic summation of analog signals. The structure consists primarily of:

a. a sensing array of MIS capacitors, called photo-gates,

b. two CCD shift registers on either side of the line sensing devices,

c. a dual transfer gate system to control the direction in which the signal charge flows out from the sensor area.

When an image is projected on the sensing elements, electron-hole pairs are generated. The electrons (in a p-type semiconductor substrate) will be normally recombined within a diffusion length from their generation sites in the deflection regions formed under the photogates. By independently adjusting the surface potential under the transfer gates, one is able to limit the diffusion and to transfer the stored charges from under the sensors (e.g., photogates) onto the desired CCD register for subsequent mathematical operations.

Binary Convolution

The implementation of a discrete convolution will now be considered in detail. The two sequences can be easily represented (1) as the input signal $e_i(t)$ in the form of charge packets generated and stored under each sensing element and (2) as a digital pattern of

narrow pulses W_k applied to the transfer gates. The convolution of these two functions or sequences yields a third one which is mathematically described as the superposition of the effect of past input excitations to account for the present output. If one assumes that the device under consideration has not reached saturation, i.e., the different potential wells are not completely filled, the output is expressed directly in terms of an explicit summing operation upon the input. Thus, the present value of the output is a weighted sum over the history of the input $e_i(t)$.

The explicit input-output relationship is:

$$e_o(t) = [W_o e_i(t) + W_1 e_i(t-T) + W_2 e_i(t-2T) + \ldots]$$

or in other notation

$$e_o(t) = \sum_{k=o}^{N} W_k e_i(t-kT)$$

where W_k is the weighting function associated with the kth position of the pulse in the timing sequence. In the present case, the weights W_k are treated as binary numbers $+$ or -1. The output is thus a weighted sum of the image samples with coefficients $+$ or -1.

The fundamental building block shown in Fig. 4 provides an output signal $e_o(t)$ as expected from equation (1) — that is the product of the sensing element signal and a parameter set by the digital timing sequence applied to the transfer gates and is algebraically summed at the output of the CCD shift registers to account for past excitations. The convolution operation is thus seen to be resulting from a series of shifting, multiplication by a weighted constant and summation. This is illustrated in Figure 5 which shows how an image is convolved with a digital pattern. The four images a, b, c, and d which constitute the input signal $e_i(t)$ illuminate four adjacent photogates as depicted in Figure 6(a). The result of applying the weighting sequence W_k described by the digital pattern 1,1,1,1 is shown in Fig. 6(b). The weighting sequence is decomposed into two timing sequences to be applied appropriately to the transfer gates. The resulting output convolutions or correlations are shown in Fig. 6(c) for two assumed illuminations a=b=c=d=1 and a=b=d=1, c=0.

E-7

Amplitude-weighted Convolution

The above example dealt with binary patterns which were defined by the timing diagram relative to both transfer gates. Integration time or pulse position affect the number of generated carriers which are stored in the sensing MIS elements. Pulse width and pulse amplitude control the partial or total transfer of the carriers from the sensor potential wells into the CCD shift registers. Thus, the mechanism by which the charges spill over into the CCD shift registers for signal processing is controlled by one or more of these parameters: integration time, pulse width and pulse amplitude:

a. The integration time is the time needed to generate sufficient number of carriers to adequately characterize the object (signal) to be measured. During integration time, the photogate is energized, thus forming a depletion layer under it to attract, capture and hold the photon generated minority carriers. The number of these carriers is proportional to the integration time, the intensity is the signal and the illuminated area.

b. The surface potential established under the transfer gate electrode is proportional to the pulse amplitude applied to the gate. Narrowing the pulse width with or without an amplitude reduction results in restricting the flow of charges out from their storage area. Widening the pulse and/or increasing the pulse amplitude has the effects of totally emptying the MIS depletion regions.

A crucial deficiency appears in mechanism (b) when compared to the first one as it leaves a fraction of the signal in the sensor area. This unused portion of signal when added to subsequent signals, will interfere with the desired device characteristics. There is however a means to remove the left-over charges: by negatively biasing the photogates to bring them into accumulation. During the process of accumulation, majority carriers (holes) are drawn to the Si/S_iO_2 interface to be recombined with the signal carriers (electrons). The mechanism of recombination is however slow in a high carrier lifetime material as is the usual case for charge transfer.

Mechanism (a), when implemented yields a more efficient operation as it transfers all available charges to the processing CCD's. Assuming that the saturation level of the potential under the photogates is not reached, one is able to adjust the fraction of the well to be filled

by controlling the integration time, i.e. by adjusting the pulse position between points t_1 and t_2 of Figure 7. Subdividing the integration time into "n" equal time intervals, the signal $e_i(t)$ can be measured down to "n" levels. The error will be commensurate with the proportion of carriers generated during the dead time from t_1 to t_2 which should therefore be at most one hundreth of the integration time in order to provide tap weights accurate to one percent. The emphasis is thus on pulse position variation to control the level of the sensed signal down from its maximum amplitude. The four images a,b,c,and d which constitute the input signal $e_i(t)$ illuminate four adjacent photogates as depicted in Fig. 8(a). The result of applying the weighting sequence W_k described by the digital pattern $1,\frac{1}{2},\bar{\frac{1}{4}},\frac{3}{4}$ is shown in Fig. 8(b). The weighting sequence is decomposed into two timing sequences to be applied appropriately to the transfer gates. The resulting output is shown in Fig. 8(c) for the assumed illumination $a=b=c=d=1$.
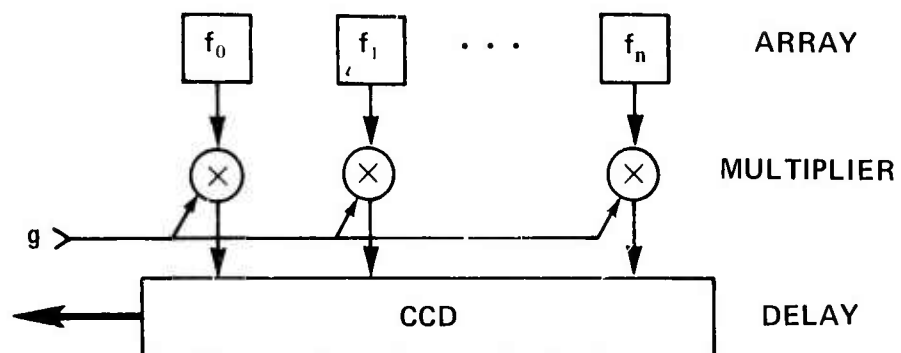
Figure 1. Block Diagram for a Signal Processing Array

OPTICAL INPUT

SPATIALLY UNIFORM   TIME VARYING

APPLICATION

OPTICAL CORRELATOR
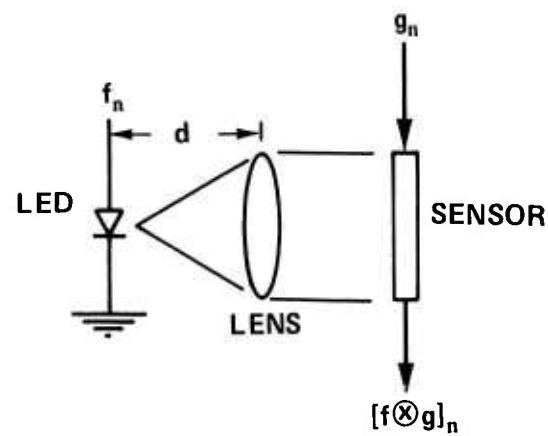
Figure 2. Configuration for an Optical Correlator/Filter

OPTICAL INPUT

{ **SPATIALLY VARIABLE**   **TIME INVARIANT**

{ **APPLICATION**

IMAGE ENCODING
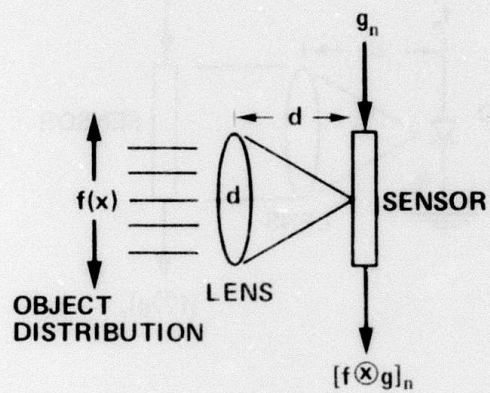
Figure 3.   Configuration for an Image Encoder

E-12
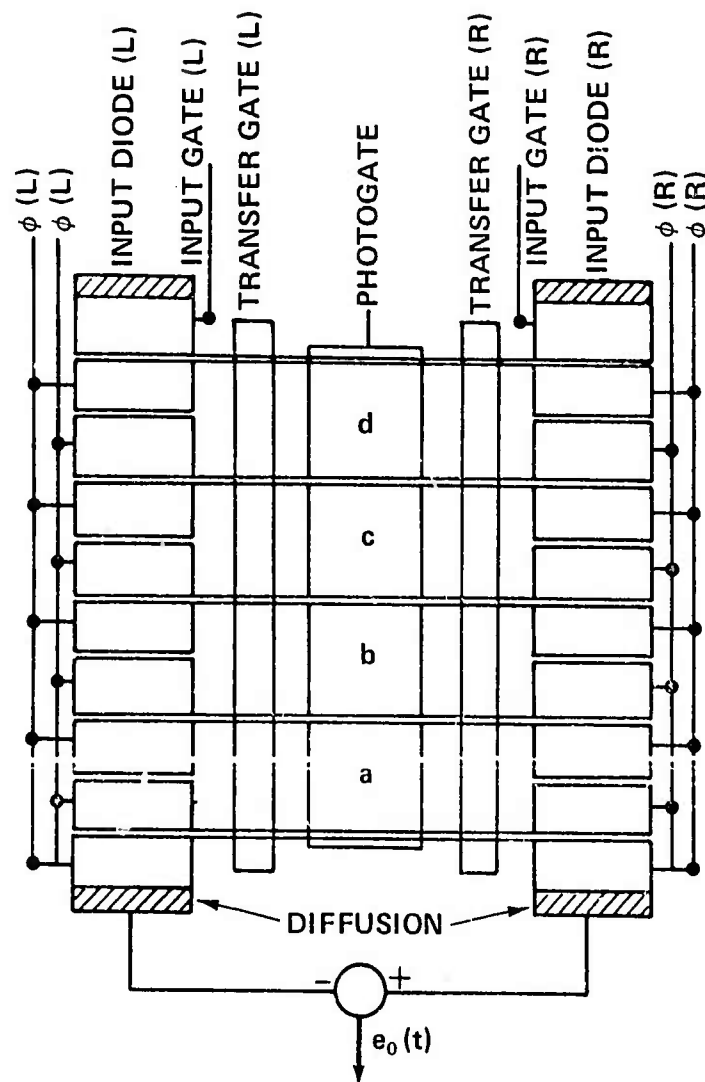
Figure 4. Mechanization of Convolution/Correlation
Operations with Charge-Coupled Devices

(a) IDEALIZED CONFIGURATION OF THE DEVICE

Figure 5. Mechanization of Convolution/Correlation Operations with Charge-Coupled Devices
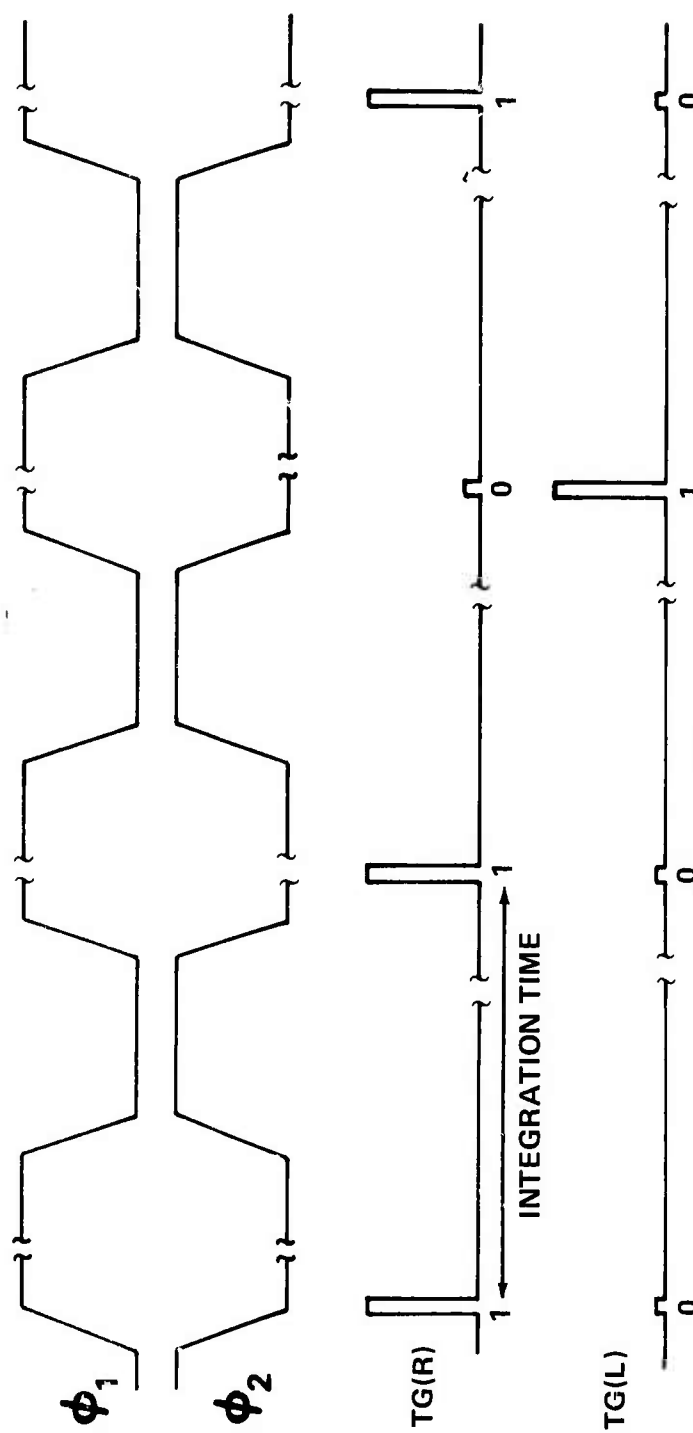
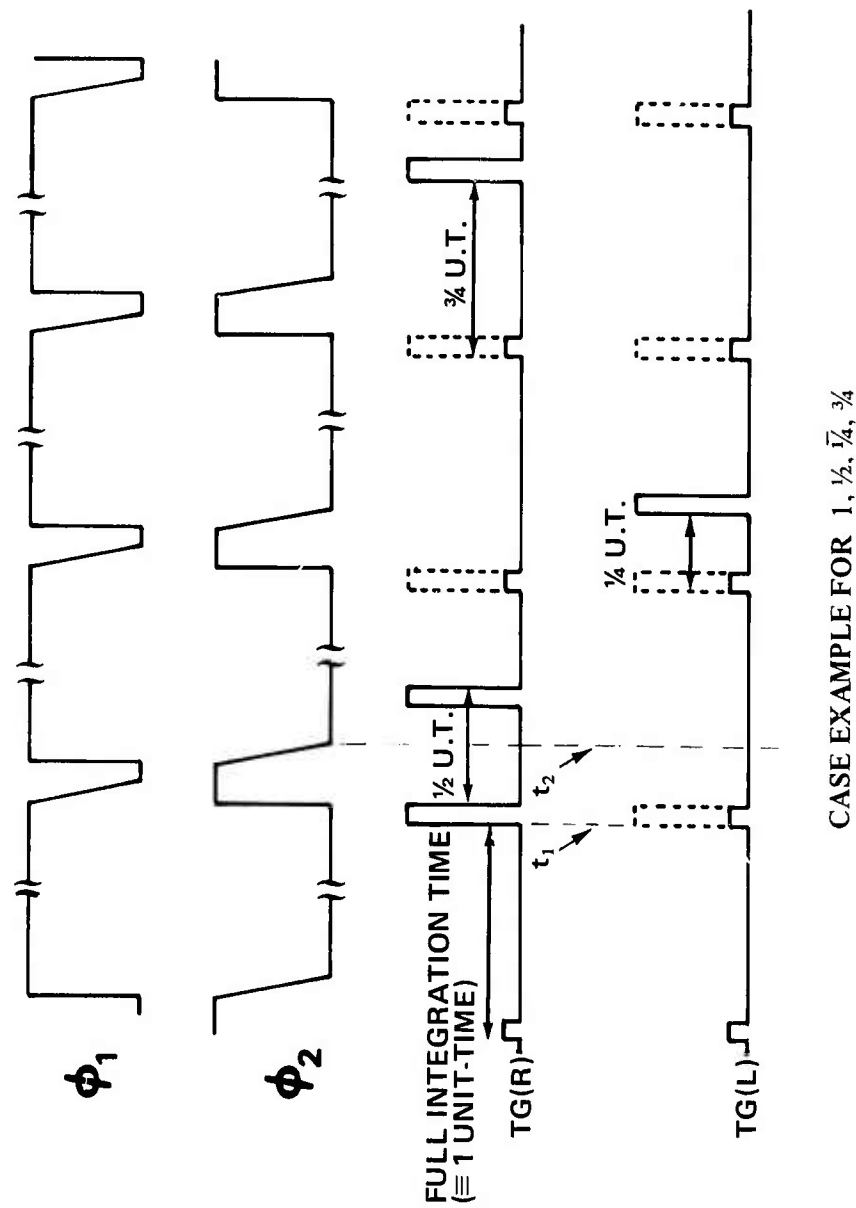Figure 5(a). Clock Phase/Transfer Gate Timing Relationship

CASE EXAMPLE FOR $1, 1, \bar{1}, 1$

(a) RESULT OF CONVOLUTION OPERATION

(b) OUTPUT OF DEVICE AT EQUAL TIME INTERVALS $t_1, t_2, \ldots, t_7$
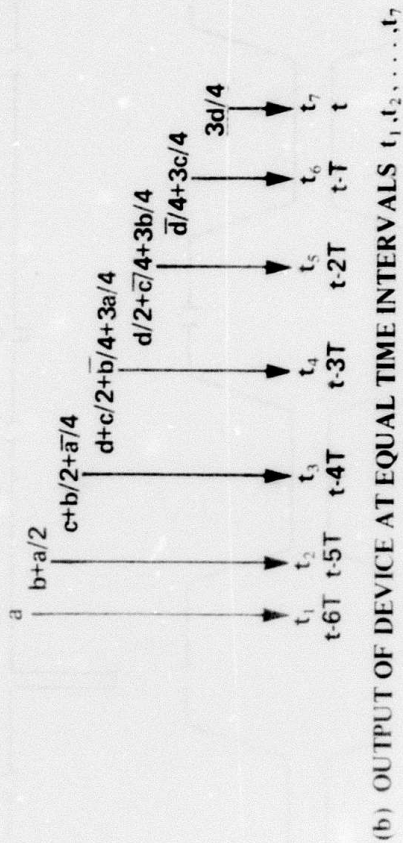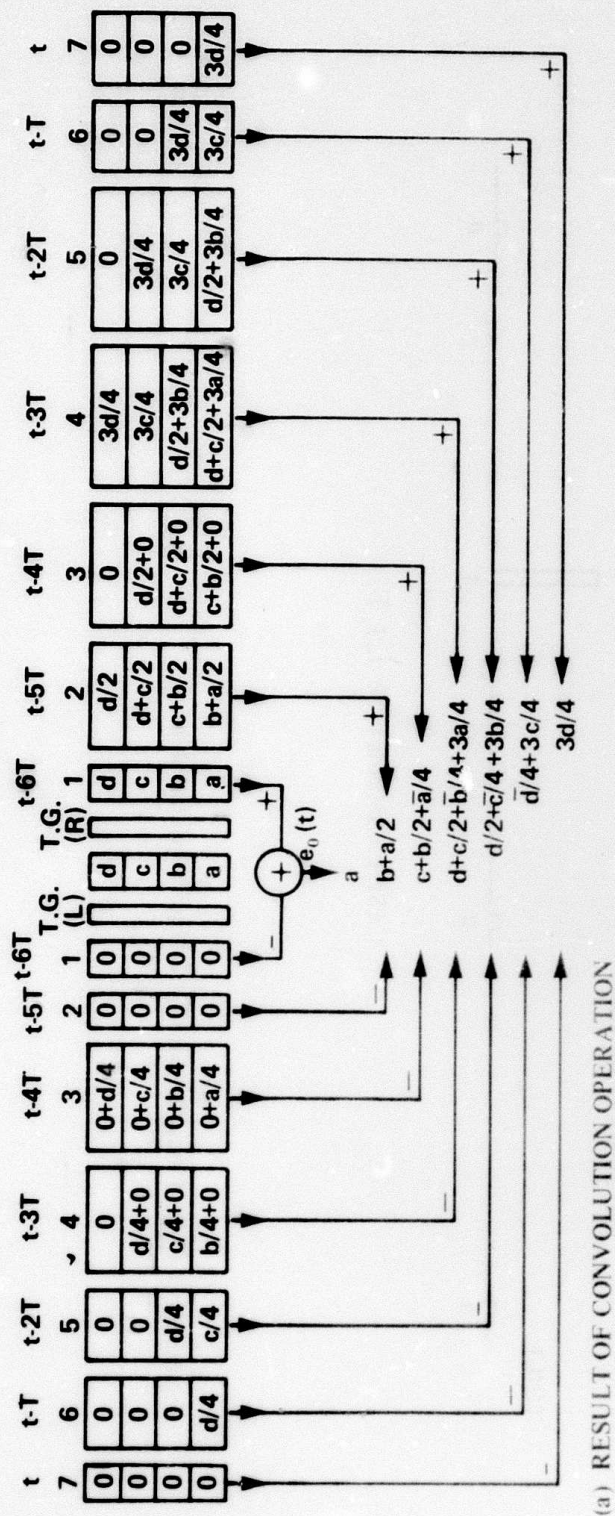
Figure 6(a) and 6(b). Illustration of Device Operation with Fractions

E-16
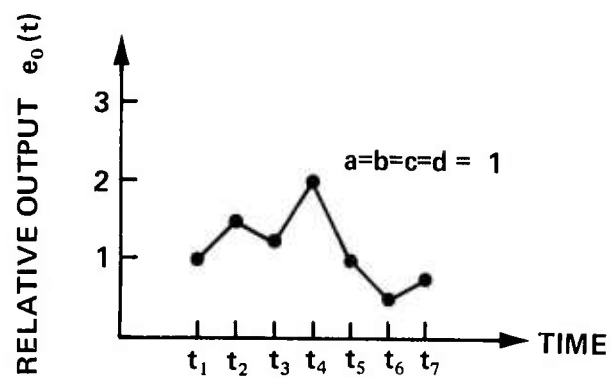
(c) RELATIVE OUTPUT VERSUS TIME

Figure 6(c). Illustration of Device Operation with Fractions

E-17
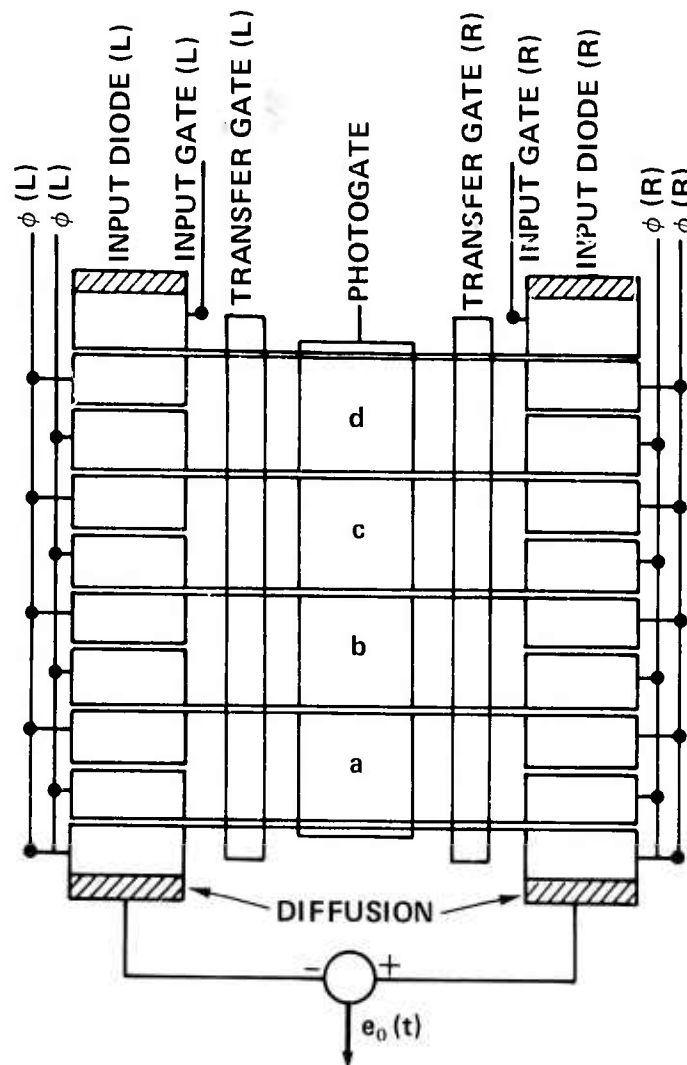
(a) IDEALIZED CONFIGURATION OF THE DEVICE
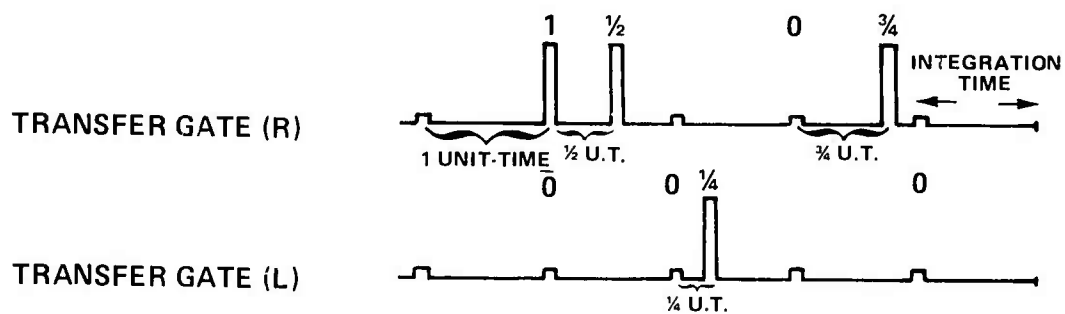
Figure 7. Mechanization of Convolution/Correlator Operations with Fractions

Figure 7(a). Clock Phase/Transfer Gate Timing Relationship for Case of Pulse Position Modulation
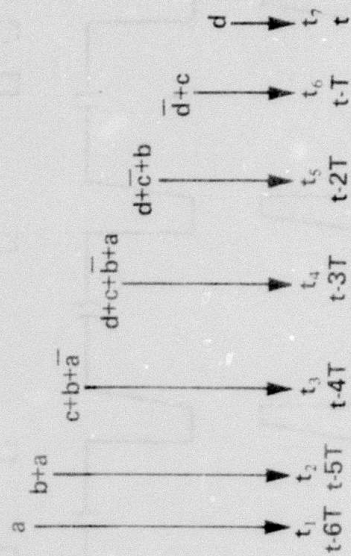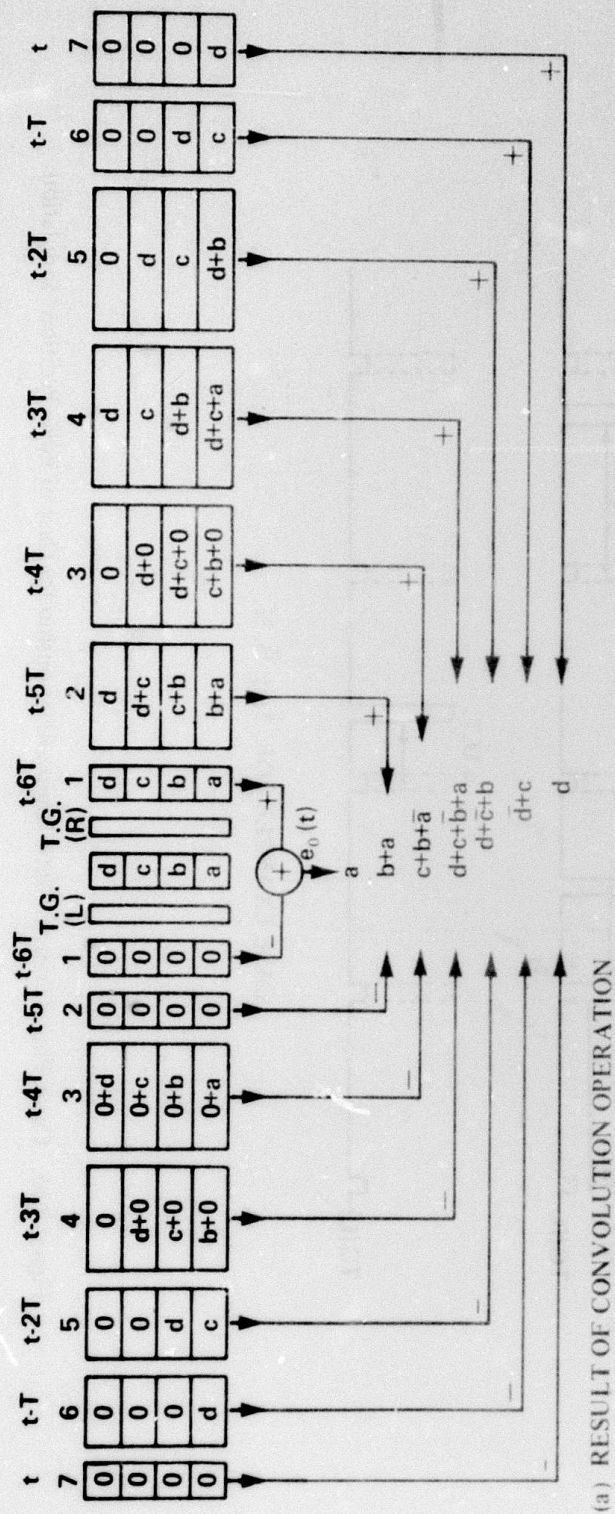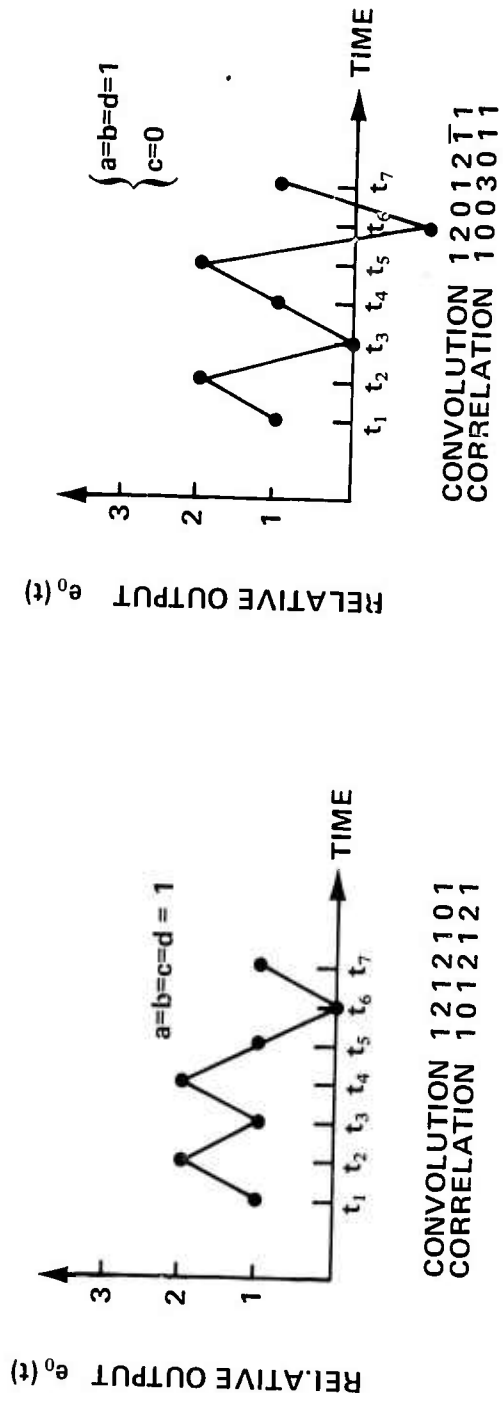
(a) RESULT OF CONVOLUTION OPERATION

(b) OUTPUT OF DEVICE AT EQUAL TIME INTERVALS $t_1, t_2, \ldots, t_7$

Figure 8(a) and 8(b).   Illustration of Device Operation

Figure 8(c). Illustration of Device Operation

BIBLIOGRAPHY

Bracewell, R. *The Fourier Transform and Its Applications.* McGraw-Hill, New York. 1965

Bromley, K. *An Optical Incoherent Correlator.* **Optica-Acta** (in press)

Gold, B. and C. M. Rader. *Digital Processing of Signals.* McGraw-Hill, New York. 1969

Pratt, W. K. and N. C. Andrews. "Application of Fourier-Hadamard Transformation to Bandwidth Compression", *Picture Bandwidth Compression.* Edited by Thomas S. Huang and OHL J. Tretiak. (pp 545 - 554) Gordon and Breach, New York. 1972

Squire, W. D., H. J. Whitehouse, and J. M. Alsup. "Linear Signal Processing and Ultrasonic Transversal Filters", *IEEE Transactions on Microwave Theory and Techniques,* **MTT - 17, No. 11**. November, 1969